



Published in final edited form as:

J Immunol. 2015 June 1; 194(11): 5211–5222. doi:10.4049/jimmunol.1401844.

Critical role of mast cells and peroxisome proliferator-activated receptor gamma (PPAR γ) in the induction of myeloid-derived suppressor cells by marijuana cannabidiol *in vivo*

Venkatesh L. Hegde¹, Udai P. Singh¹, Prakash S. Nagarkatti¹, and Mitzi Nagarkatti^{1,2}

¹Department of Pathology, Microbiology and Immunology, University of South Carolina School of Medicine, Columbia, SC 29208, United States

²WJB Dorn Veterans Affairs Medical Center, Columbia, SC 29208, United States

Abstract

Cannabidiol (CBD) is a natural non-psychoactive cannabinoid from marijuana (*Cannabis sativa*) with anti-epileptic and anti-inflammatory properties. Effect of CBD on naïve immune system is not precisely understood. In this study, we observed that administering CBD into naïve mice triggers robust induction of CD11b⁺Gr-1⁺ MDSC in the peritoneum, which expressed functional Arg1, and potently suppressed T cell proliferation *ex vivo*. Further, CBD-MDSC suppressed LPS-induced acute inflammatory response upon adoptive transfer *in vivo*. CBD-induced suppressor cells were comprised of CD11b⁺Ly6-G⁺Ly6-C⁺ granulocytic and CD11b⁺Ly6-G⁻Ly6-C⁺ monocytic subtypes, with monocytic MDSC exhibiting higher T cell suppressive function. Induction of MDSC by CBD was markedly attenuated in Kit-mutant (Kit^{W/W^{-v}}) mast cell-deficient mice. MDSC response was reconstituted upon transfer of WT bone marrow-derived mast cells in Kit^{W/W^{-v}} mice suggesting the key role of cKit (CD117) as well as mast cells. Moreover, mast cell activator compound 48/80 induced significant levels of MDSC *in vivo*. CBD administration in mice induced G-CSF, CXCL1 and M-CSF, but not GM-CSF. G-CSF was found to play a key role in MDSC mobilization inasmuch as neutralizing G-CSF caused a significant decrease in MDSC. Lastly, CBD enhanced the transcriptional activity of PPAR γ in luciferase reporter assay, and PPAR γ selective antagonist completely inhibited MDSC induction *in vivo* suggesting its critical role. Together, the results suggest that CBD may induce activation of PPAR γ in mast cells leading to secretion of G-CSF and consequent MDSC mobilization. CBD being a major component of Cannabis, our study indicates that marijuana may modulate or dysregulate the immune system by mobilizing MDSC.

Keywords

Arginase; rodent; mice; cytokine; chemokine; cannabidiol; myeloid-derived suppressor cells; PPAR γ ; miRNA; mast cell; G-CSF

INTRODUCTION

Cannabidiol (CBD) is the major constituent of marijuana (*Cannabis Sativa*) plant, constituting up to 40% in some preparations (1). Unlike THC, CBD is non-psychotropic and has attracted a lot of interest as a promising therapeutic for various clinical disorders. CBD is known to possess analgesic, anti-emetic and anti-inflammatory properties. CBD is also a potent anti-oxidant with significant neuroprotective action (2–6). CBD, along with natural THC, is the main component of Sativex®, an oromucosal spray approved for clinical use in Germany, UK, Canada and other countries to alleviate spasticity and neuropathic pain in MS patients (7, 8), and recently under consideration for FDA approval for the treatment of pain in cancer patients in United States. Recently, CBD has also been approved by the FDA for preliminary studies to treat intractable epilepsy in children.

Myeloid-derived suppressor cells (MDSC) are a heterogeneous population of myeloid cells that are believed to be arrested at an immature state of cell differentiation, meanwhile acquiring potent immunosuppressive function (9–13). MDSC are defined by their myeloid origin, immature state and ability to potently suppress T cell responses. These cells found in small numbers in a healthy state, are known to rapidly expand in response to cancer, during infections and inflammation. MDSC have been investigated as a potential therapeutic target to promote anti-tumor immune responses or to suppress immune responses during autoimmune inflammation and transplantation (10, 12, 14, 15).

The potent anti-inflammatory and immunomodulatory effects of cannabidiol has been demonstrated in various pre-clinical disease models such as murine collagen induced arthritis (16), high glucose-induced endothelial cell inflammatory response and barrier disruption (17), β -amyloid induced neuroinflammation (18), acute carrageenan-induced inflammation (19), development of type I diabetes in NOD mice (20), hepatic ischemia/reperfusion injury (21), LPS-induced inflammation in brain (22) and MS like disease (23). In line with its wide spectrum of action, CBD has been shown to bind to various receptors such as vanilloid receptor (Trpv1), cannabinoid receptors (CB1 and CB2), Adenosine receptor 2A (A2A), α -1 and α -1- β glycine receptors (18) with varying affinities, and has been shown to function via different receptors in different models. Recent studies demonstrated that CBD directly activates peroxisome proliferator-activated receptor PPAR γ , a non-cannabinoid nuclear receptor, to influence gene expression (24–26) and exert its effects. Although, CBD is shown to decrease T cell responses and inhibit inflammatory cytokine production in these models, little is known about the effect of CBD on important suppressor cell populations. Recently, we showed that CBD was able to ameliorate T cell-mediated acute liver inflammation in ConA-induced as well as D-Galactosamine/Staphylococcal Enterotoxin B (D-Gal/SEB)-induced hepatitis in mice, which was associated with significant increase in MDSC in livers (27). Because inflammation is also known to trigger MDSC, it was not clear from these studies if CBD further augmented the inflammation-driven MDSC induction.

In the current study, therefore, we investigated if administration of CBD into normal mice would induce MDSC. Interestingly, we found that CBD caused robust induction of immunosuppressive CD11b⁺Gr-1⁺ MDSC in naïve mice which was associated with

significant upregulation of G-CSF, M-CSF and CXCL1. We demonstrate that this response is dependent on mast cells, and primarily mediated by PPAR γ .

MATERIALS AND METHODS

Mice

Female C57BL/6 mice and TLR4-mutant C₃H/HeJ (Tlr4^{Lps-d}) mice, 8–12 weeks old were purchased from National Cancer Institute (Frederick, MD). Female vanilloid receptor knockout mice on BL/6 background (B6.129X1-Trpv1^{tm1Jul}/J), and mast cell-deficient mice (WBB6F1/J-Kit^W/Kit^{W-v}) and their WT (+/+) littermate controls were purchased from The Jackson Laboratory (Bar Harbor, ME). Mice were housed under standard pathogen-free conditions in the Animal Resource Facility of University of South Carolina School of Medicine and all experiments were conducted after obtaining prior approval from the Institutional Animal Care and Use Committee.

Reagents

Cannabidiol, SR141716A (SR1, CB1 antagonist) and SR144528 (SR2, CB2 antagonist) were provided by National Institute of Drug Abuse. The monoclonal antibodies (mAbs), FITC-conjugated anti-CD11b (clone: M1/70), anti-Ly6C (HK1.4), PE-conjugated anti-Gr-1 (anti-Ly6G/Ly6C, clone: RB6-8C5), anti-Ly6G (clone: IA8), anti-CD3, anti-CD4, anti-CD8, anti-CD31, anti-CD11c, anti-F/480, anti-Ki-67, Alexa 647-conjugated anti-CD11b and purified anti-CD16/CD32 (mouse Fc receptor block) were from Biolegend (San Diego, CA). The anti-arginase Ab was obtained from BD Transduction Laboratories. The anti-Gr-1 microbeads, magnetic sorting columns and equipment were from Miltenyi Biotech. Adenosine (A_{2A}) receptor antagonist 4-(2-[7-Amino-2-(2-furyl)[1,2,4]triazolo[2,3-a][1,3,5]triazin-5-ylamino]ethyl)phenol (ZM 241385), PPAR γ antagonist 2,2-Bis[4-(2,3-epoxypropoxy)phenyl]propane (Bisphenol A diglycidyl ether or BADGE) and PPAR γ agonist 5-[[4-[(3,4-Dihydro-6-hydroxy-2,5,7,8-tetramethyl-2H-1-benzopyran-2-yl)methoxy]phenyl]methyl]-2,4-thiazolidinedione (troglitazone) were purchased from Tocris Bioscience. Cell culture grade concanavalin A, L-arginine, L-ornithine standard, Ninhydrin reagent, red blood cell lysis buffer and all other chemicals and reagents were from Sigma-Aldrich (St. Louis, MO).

Administration of compounds and preparation of cells

Mice were injected with CBD at different doses intraperitoneally. DMSO stock of CBD was diluted in sterile PBS and solubilized using a small amount of Tween-80. DMSO and Tween-80 similarly diluted in PBS at a ratio of 94:4:2 (PBS:DMSO:Tween-80) was used as the vehicle. The concentration of DMSO and Tween-80 in the vehicle was <3.2% and <2% respectively. Exudates cells in the peritoneal cavity were harvested after 12 or 24 h by performing peritoneal lavage with sterile, ice cold PBS (5mL \times 3), as described previously (28). Bone marrow cells were obtained by flushing tibia with ice cold PBS followed by RBC lysis. For *in vivo* blocking experiments, SR1, SR2 compounds, ZM 241385, BADGE, control IgG or anti-G-CSF Ab were injected i.p. at the indicated doses 1 h prior to injecting CBD. For thioglycolate (TG)-induced neutrophil response, 0.5 mL of 3% TG broth was injected intraperitoneally and cells were harvested 4 h or 16 h post-injection.

Immunofluorescence staining and flow cytometry

For fluorescence-activated cell sorting (FACS) analysis, cells were blocked using mouse Fc-block and stained for cell surface markers using fluorescently labeled mAbs (10 µg/mL) (28). After washing, stained cells were analyzed in a flow cytometer (Beckman Coulter). Isotype antibody-treated cells served as staining controls. Data obtained were analyzed in Cytomics CXP software (Beckman Coulter).

Cell lysates

Cell lysates were prepared by suspending the cell pellet in lysis buffer (50 mM HEPES, 150 mM NaCl, 5 mM EDTA, 1 mM NaVO₄, and 0.5% Triton) containing 50 µg/ml aprotinin, 50 µg/ml leupeptin, 100 µg/ml trypsin-chymotrypsin inhibitor, and 2 mM PMSF. Lysates were centrifuged at 12000×g for 5 min at 4°C. Protein content was determined by BCA method (Pierce).

Western Blotting

Cell lysates (20µg protein per lane) were separated by SDS-PAGE and electrophoretically transferred onto nitrocellulose membrane using a semi-dry transfer unit (Bio-Rad) followed by blocking with 5% blotting grade dry milk in tris-buffered saline containing 0.1% tween-20. Next, membranes were incubated with anti-mouse-arginase (1:2000), washed and probed with anti-mouse HRP secondary antibody (1:15000). The blots were developed using ECL reagent (GE) on to Kodak BioMax chemiluminescence film. β-actin was used as the internal control.

Arginase Activity Assay

Arginase activity in the cell lysates were determined as described previously (28) by measuring the production of L-ornithine and urea. Briefly, cell lysates were added to Tris-HCl (50mM, pH 7.5) containing 10mM MnCl₂ and the mixture was heated at 55–60°C for 10 min to activate arginase. Then, a solution containing carbonate buffer (100 mM) and L-arginine (100mM) was added and incubated at 37°C for 20 min. The hydrolysis product L-ornithine was detected by colorimetric assay using ninhydrin reagent.

Cell sorting

MDSC were enriched by magnetic sorting using anti-Gr-1 micro beads according to manufacturer's instructions (Miltenyi Biotech). Enriched cells were found to be >90% pure for CD11b and Gr-1 expression as determined by FACS analysis. For some experiments, CD11b⁺Gr-1⁺ MDSC, granulocytic and monocytic MDSC subtypes were purified by sorting (>90% purity) on FACS Aria cell sorter (BD Biosciences) after labeling with appropriate fluorescently conjugated mAbs.

T cell proliferation assay

Purified MDSC were irradiated at approximately 2000 rad and cultured at 1:10 and 1:2 ratios with syngenic lymph node T cells (2×10^5) in round bottom 96-well plates using complete RPMI 1640 medium supplemented with 10% FBS, 10mM HEPES, 2mM L-glutamine, 1mM penicillin-streptomycin, and 50µM β-mercaptoethanol. T cells were

stimulated with cell culture grade ConA (4 μ g/mL). Specific arginase inhibitor nor-NOHA was added (10 or 100 μ M) in some wells. T cell proliferation was assessed after 72 h culture by pulsing with [3H] thymidine (2 μ Ci/well) during the last 16 h of culture. Cells were harvested using a cell harvester and thymidine incorporation was measured in a beta counter (Perkin Elmer).

MDSC adoptive transfer and LPS-induced TNF- α production *in vivo*

Purified CBD-induced CD11b⁺Gr-1⁺ MDSC (>90% purity) were adoptively transferred to naïve WT mice (5 \times 10⁶ cells per mouse, i.v.). After 16 h, mice were injected with vehicle or LPS (1 mg/kg, i.v.). One hour after LPS administration, sera were collected by retro-orbital bleeding, and TNF- α levels were determined by ELISA (Biolegend).

Chemokine ELISA

For chemokine analysis, peritoneal exudates from vehicle or CBD-injected mice were obtained by lavage using 1 mL sterile, cold PBS. Cells were spun down and supernatants obtained were analyzed for G-CSF, M-CSF (Peprotech), GM-CSF (Biolegend), and CXCL1 (R&D System) by ELISA.

Generation of bone marrow-derived mast cells for adoptive transfer

Bone marrow-derived mast cells (BMDC) cultures were prepared as described previously (29) with minor modifications. Briefly, bone marrow cells were obtained by flushing the tibia of WT mice followed by RBC lysis. Cells were cultured in complete RPMI 1640 media supplemented with 10% heat-inactivated FBS, 25 mM HEPES (pH 7.4), 2 mM L-glutamine, 0.1 mM nonessential amino acids, 1 mM sodium pyruvate, 50 μ M 2-mercaptoethanol, 100 IU/ml penicillin–100 μ g/ml streptomycin, 10 ng/ml recombinant mouse IL-3 and 20 ng/ml recombinant mouse stem cell factor. Cells were cultured for 6 weeks, passaging every 3–4 days. Once the majority of cells in culture were non-adherent in appearance, the purity was tested by FACS analysis for c-Kit expression. BMDC with >90% purity were used for adoptive transfer into mast cell-deficient mice.

Reverse transcription-PCR for PPAR γ

RT-PCR was performed by a standard protocol (27). Total RNA was extracted using RNeasy kit (QIAGEN) followed by cDNA synthesis. The following primers were used for PCR amplification: Pparg transcript variant 1 (forward, 5'GGA AGA CCA CTC GCA TTC CTT3'; reverse, 5'GTA ATC AGC AAC CAT TGG GTC A3') and internal control 18S (forward, 5'GCC CGA GCC GCC TGG ATA C3'; reverse, 5'CCG GCG GGT CAT GGG AAT AAC3'). The PCR products were analyzed by 1.5% agarose gel electrophoresis in the presence of ethidium bromide and photographed using a gel imager (Bio-Rad).

Luciferase reporter Assay

P815 murine mast cells were transfected with PPAR luciferase reporter using SuperFect transfection reagent (Qiagen) in Opti MEM® medium. PPAR reporter used for transfection was a mixture of a PPAR-responsive (inducible) *Firefly* luciferase construct and a constitutively expressing *Renilla* luciferase construct. A constitutively expressing GFP

construct was used initially to optimize transfection conditions for P815 cells (~62%). After 24 hours of transfection, cells were treated with vehicle (control), CBD or a positive control PPAR γ agonist, troglitazone. For in vitro assays the vehicle for CBD contained <0.1% DMSO at final concentrations. Luciferase assay was performed 24 hours following treatment using a commercially available Dual-Glo[®] luciferase assay system (Promega) and measured in a luminometer (Perkin Elmer). Values were expressed as normalized relative luciferase units and fold induction compared to control was calculated.

Statistical Analysis

Data are expressed as mean \pm SD. In most in vivo experiments, we used 3–6 mice for each treatment group, unless otherwise mentioned. Student's *t*-test was used for comparing two groups and a *P* value of 0.05 was considered as statistically significant. At least two replicate experiments were performed to test the reproducibility of results.

RESULTS

CBD induces CD11b⁺Gr-1⁺ cells *in vivo*

To investigate the cellular response to CBD in naïve mice, we injected groups of C57BL/6 mice (WT) intraperitoneally with a single dose of 20 mg/kg bd. wt. of CBD, and harvested the exudate cells from the peritoneum after various time points (0–48 hours). We analyzed the peritoneal exudate cells for the co-expression of CD11b and Gr-1 antigens by flow cytometry. We found that compared to a small percentage in the control mice, a significant proportion of the cells induced by CBD in the peritoneum co-expressed CD11b and Gr-1 at 6, 12 and 24 h (Fig. 1A). Determination of absolute CD11b⁺Gr-1⁺ cell numbers based on frequency and total viable cells per peritoneum showed a significant and robust induction in their numbers in time-dependent manner from 6–24 h with a sharp decrease by 48 h (Fig. 1B). The cellular response was found to peak at 24 h and sharply decrease by 48 h (Fig. 1B). Next, to determine if this cellular response to CBD is dose-dependent, we injected WT mice with vehicle or different doses of CBD (1, 10, 20 mg/kg), and analyzed the cells harvested from peritonea after 16 h. Administration of CBD resulted in robust, dose-dependent increase in the frequency (Fig. 1C) as well as absolute number (Fig. 1D) of CD11b⁺Gr-1⁺ cells. To test the possible involvement of TLR4 and effect of any contaminating LPS that may be present in the CBD preparation, we injected TLR4-mutant C₃H/HeJ (*Tlr4^{Lps-d}*) mice unresponsive to bacterial endotoxin (30) with the same batch of CBD or vehicle and analyzed the peritoneal cells after 12 hours as above. CBD induced significant number of CD11b⁺Gr-1⁺ cells in TLR4-mutant mice, similar to WT mice (Fig. 1E, F) suggesting that the observed induction of MDSC by CBD is independent of any TLR4-mediated mechanisms.

Next, we compared the in vivo cellular response to CBD side-by-side with that of typical acute inflammatory response to thioglycollate (TG) broth in the peritoneum. TG broth is known to cause a neutrophil predominant response at a very early time point (2–6 h) in the peritoneum followed by monocyte accumulation after 48–72 h (31). Compared to CBD-induced MDSCs which expressed intermediate levels of Gr-1 antigen, TG-induced neutrophils showed higher expression of Gr-1 (Fig 2A). Notably, TG-neutrophils

consistently showed >10 fold higher expression of Gr-1 compared to CBD MDSC as determined by mean fluorescence intensities in FACS analysis (Fig 2B). The Gr-1⁺ cells induced by CBD and TG were enriched by magnetic sorting and used in T cell proliferation assay using syngenic lymph node T cells stimulated polyclonally with ConA. Gr-1^{high} neutrophils induced by TG did not cause a decrease in T cell proliferation whereas, CBD-induced Gr-1^{int} MDSCs exhibited marked inhibition of T cell proliferation (Fig 2D).

***In vivo* CBD-induced CD11b⁺Gr-1⁺ cells are immunosuppressive MDSC**

CBD-induced CD11b⁺Gr-1⁺ cells express functional Arginase—In order to test if the CD11b⁺Gr-1⁺ cells induced by CBD *in vivo* were MDSC, we first analyzed the cells for the expression of functional arginase 1 (Arg1), a characteristic functional marker of MDSC. Lysates of cells harvested from peritoneum of WT mice injected with vehicle or CBD were subjected to Western blot analysis (Fig. 3A). Cells from the peritoneum of CBD-injected mice showed increased arginase expression compared to that of vehicle. Cell lysates were also analyzed for Arg1 activity by spectrophotometric assay (Fig. 3B). As shown, peritoneal exudate cells from CBD-injected mice showed significantly higher Arg1 compared to cells from vehicle treated mice.

CBD-induced CD11b⁺Gr-1⁺ cells suppress T cell proliferation ex vivo—We purified CD11b⁺Gr-1⁺ cells from the peritoneum of CBD-injected mice, and co-cultured them with syngenic T cells stimulated with ConA at 1:10 and 1:2 MDSC:T cell ratios (Fig. 3C). T cells stimulated with ConA and cultured without MDSC served as the positive control. T cell proliferation was assessed by radioactive thymidine incorporation. CBD-induced CD11b⁺Gr-1⁺ cells significantly decreased T cell proliferation, almost completely inhibiting at 1:2 MDSC:T cell ratio. Furthermore, co-incubation with increasing concentrations of arginase inhibitor nor-NOHA was able to block the suppressive activity of MDSC. These results established that CD11b⁺Gr-1⁺ cells induced by CBD *in vivo* were highly immunosuppressive, functional MDSC.

Adoptively transferred CBD-induced MDSC suppress acute inflammation—To assess the suppressive activity of CBD-induced MDSC *in vivo* following adoptive transfer, we used the classical lipopolysaccharide model of acute inflammatory (TNF- α) response. We purified CD11b⁺Gr-1⁺ cells from the peritoneum of mice injected with CBD, and transferred them into WT mice before challenging with LPS. The acute inflammatory response was assessed by measuring TNF- α levels in the sera 1 h post-LPS challenge. Mice injected with LPS showed very high levels of TNF- α in their sera compared to control mice. Whereas, mice transferred with CBD-induced CD11b⁺Gr-1⁺ MDSC showed significantly decreased levels of serum TNF- α (Fig. 3D) demonstrating the potent suppressive nature of these cells.

CBD causes mobilization of CD11b⁺Gr-1⁺ cells from bone marrow

Naïve mice have small numbers (<5%) of CD11b⁺Gr-1⁺ cells in peripheral tissues such as spleen, whereas 18% to as high as 50% in the bone marrow (28, 32, 33). As CBD induces robust accumulation of MDSC rapidly in the peritoneum by 6–12 hours, we speculated that the cells may be migrating from bone marrow. To test this, we injected WT mice with CBD

and analyzed for CD11b⁺Gr-1⁺ cells at 0 and 12 h in bone marrow and peritoneum (Fig. 4A). Corresponding with the significant accumulation of MDSC in the peritoneum, we observed a significant decrease in the frequency of CD11b⁺Gr-1⁺ cells in the bone marrow 12 h following exposure to CBD. This indicated that CD11b⁺Gr-1⁺ cells were migrating from bone marrow in response to CBD. Further, CBD-induced MDSC from peritoneum showed expression of immature myeloid marker CD31 and were found to be actively dividing based on positive Ki-67 staining (Fig. 4B). These results suggested that CBD-induced MDSCs from peritoneum are immature, actively proliferating myeloid cells, directly derived from BM myeloid precursors rather than reprogrammed, terminally differentiated myeloid population.

In addition to peritoneum, we assessed the cellular response in spleen in CBD-injected mice. We saw a significant increase in CD11b⁺Gr-1⁺ cell numbers in spleen (Fig. 4C, D), indicating that CBD causes significant accumulation of MDSCs not only locally but other organs in the periphery such as spleen. Phenotyping of cells from the peritoneal cavity of mice injected with CBD or vehicle was carried out (Fig. 4E). CBD administration did not alter the number of T lymphocytes as shown by CD3, CD4 and CD8 staining. In addition to dramatic increases in CD11b⁺ and Gr-1⁺ cells, there was a small but significant increase in CD11c⁺ dendritic cells in CBD-injected peritonea. However, the classical F4/80(high) macrophages which are found in significant numbers in the control peritoneum were decreased with CBD. Unlike F4/80(high)-macrophages, MDSC have been shown to express low to intermediate levels of F4/80. Accordingly, we saw F4/80^{low/int} expressing cell numbers dramatically increased in CBD-peritoneum comparable to the levels of CD11b⁺ and Gr-1⁺ cells. Triple staining with these markers has further confirmed the low/int expression of F4/80 on CD11b⁺Gr-1⁺ MDSCs (data not shown).

Characterization of CBD-induced MDSC subtypes

CD11b⁺Gr-1⁺ MDSC mainly comprise of two major subtypes, namely granulocytic and monocytic MDSC. To characterize CBD-induced MDSC subtypes, we injected WT mice with vehicle or CBD and harvested peritoneal exudate cells after 16 hours. Cells were triple-stained for CD11b, Ly6-G and Ly6-C and analyzed by flow cytometry. Cells were gated for CD11b⁺ expression and analyzed for Ly6-G and Ly6-C. CBD induced significant accumulation of CD11b⁺Ly6-G⁺Ly6-C^{+(int)} granulocytic (Gr) and CD11b⁺Ly6-G^{-(neg)}Ly6-C⁺ monocytic (Mo) MDSC subtypes as compared to vehicle (Fig. 5A, B). Based on the frequency as well as absolute numbers, the two subsets were induced at similar levels. Next, to compare their T cell suppressive efficacy, Gr- and Mo- MDSC induced by CBD were purified by FACS sorting (>90%) and used in T cell suppression assay with syngenic T cells stimulated with ConA. While both the subsets decreased the T cell proliferation markedly at both 1:100 and 1:10 MDSC:T cell ratios, monocytic subtypes inhibited T cell proliferation to a significantly greater extent than the granulocytic MDSC indicating that monocytic MDSC induced by CBD were significantly more immunosuppressive than their granulocytic counterparts (Fig. 5C).

Critical role of c-Kit and mast cells in the induction of MDSC by CBD

To test the role of mast cells in CBD-induced mobilization of MDSC, we used c-Kit mutant Kit^W/Kit^{W-v} mice and their wild-type (+/+) littermates as controls. Wild-type littermate controls (+/+) showed significant induction of CD11b⁺Gr-1⁺ cells in response CBD in the peritoneum as compared to vehicle, whereas, Kit^W/Kit^{W-v} mice showed decreased frequency of MDSC (Fig. 6A), and dramatically attenuated total MDSC numbers in the peritoneum in response to CBD compared to WT (Fig. 6B). Analysis for MDSC subsets in these experiments showed that while the frequency of Gr-MDSC decreased by half, that of Mo-MDSC decreased by more than 4 fold in Kit^W/Kit^{W-v} mice compared to controls in response to CBD suggesting that c-Kit deficiency attenuated the induction of monocytic MDSC to a higher extent than granulocytic subtype (Fig. 6C).

Induction of MDSC by CBD *in vivo* is associated with the upregulation of G-CSF, CXCL1 and M-CSF but not GM-CSF

We analyzed the chemokine response to CBD in the peritoneum to identify the important chemokine mediators associated with the induction of MDSC. G-CSF and GM-CSF have been previously shown to play important roles in the development and induction of MDSC (34, 35). We analyzed these chemokines in the peritoneal exudates at various time points following the administration of CBD by ELISA. G-CSF levels were markedly increased in response to CBD as early as 6 h, peaking around 12 h and starting to decrease by 48 h (Fig. 7A). We did not see any change in the levels of GM-CSF. We also determined other potential chemokines, M-CSF and KC (CXCL1) in peritoneal exudates post-CBD injection. We observed significant induction of M-CSF at 12 and 24 h (Fig. 7B) and a sharp induction of CXCL1 at 12 h (Fig. 7C) in response to CBD. These data suggested that G-CSF, CXCL1 and M-CSF may play a role in the induction of MDSC by CBD *in vivo*.

Blocking of G-CSF inhibits MDSC induction *in vivo*

Relatively more robust increase in G-CSF compared to other chemokines (Fig. 7B–C) indicated that G-CSF may be playing a more prominent role. We further investigated the role of G-CSF by *in vivo*-blocking experiment using anti-G-CSF Ab. A low dose of 10µg/mouse anti-G-CSF was able to significantly block both the frequency and the absolute numbers of MDSC induced by CBD in the peritoneum as compared to control mice pretreated with isotype IgG (Fig. 7D, E) suggesting the crucial role of G-CSF in this process.

Induction of G-CSF by CBD is c-kit-dependent

We analyzed G-CSF levels in peritoneal exudates of WT and c-Kit-mutant mast cell-deficient mice injected with CBD. Kit^W/W^{-v} mice produced significantly lower levels of G-CSF in the peritoneal exudates in response to CBD compared to control mice (Fig. 7F) suggesting that induction of G-CSF *in vivo* by CBD is c-Kit-dependent.

Adoptive transfer and replenishment of mast cells in Kit^{W/W-v} mice restores the CBD response

We sought to identify the cell type responsible for accumulation of MDSC in the peritoneum in response to CBD. The lining of the peritoneum is known to contain mast cells in significant numbers which can rapidly secrete mediators upon activation. Because the Kit^{W/W-v} mice are also deficient in mast cells, we hypothesized that mast cells may be playing an important role in the induction of MDSC in response to CBD. To further assess this, we generated mast cells from WT bone marrow by a standard six week culture in the presence of IL-3 and stem cell factor (Fig. 8A) and adoptively transferred the cultured mast cells into Kit^{W/W-v} mice. Six weeks following transfer, Kit^{W/W-v} mice with or without transferred mast cells were injected with vehicle or CBD. Enumeration of mast cells in the peritoneal lavage confirmed the replenishment of mast cells in mast cell deficient mice (Table I). Mast cell-replenished Kit^{W/W-v} mice showed a significantly increased number of CD11b⁺Gr-1⁺ cells in the peritoneum in response to CBD when compared to Kit^{W/W-v} mice without mast cell transfer (Fig. 8B, C). Furthermore, those mice also showed increased G-CSF production in the peritoneum (Fig. 8D) suggesting that adoptive transfer of mast cells in Kit^{W/W-v} mice was able to restore the MDSC response to CBD. These results suggested that mast cells may play an important role in the induction of MDSC *in vivo*.

Mast cell activator (C-48/80) induces accumulation of MDSC

To further corroborate the potential, likely role of mast cells in MDSC induction, we tested if a known mast cell activator can induce MDSC *in vivo*. To this end we injected WT mice intraperitoneally with compound-48/80 and analyzed the accumulation of MDSC in the peritoneum. C-48/80 produced a significant dose-dependent increase in the frequency and absolute number of CD11b⁺Gr-1⁺ MDSC in the peritoneum (Fig. 9A, B). Further, analysis for MDSC subtypes showed significant induction of both the granulocytic and monocytic MDSC subsets in response to mast cell activation by C-48/80 *in vivo* (Fig. 9C).

Critical role of nuclear receptor PPAR γ

To delineate the role of receptors in the induction of MDSC by CBD, we used receptor-deficient mice or specific antagonists for receptors that CBD is known to bind to and function. Ion channel receptor Trpv1 (vanilloid) has been shown to be the primary receptor for CBD in a number of *in vitro* and *in vivo* systems (1, 27, 36). First, we used vanilloid receptor-deficient (Trpv1^{-/-}) mice to study its role. We injected WT and Trpv1^{-/-} mice with vehicle or CBD and analyzed the peritoneal exudate cells after 16 h. Surprisingly, CBD administration resulted in significant induction of MDSC in Trpv1^{-/-} mice similar to Trpv1^{+/+} WT mice (Fig. 10A, B). This suggested that CBD-induced accumulation of MDSC *in vivo* in the peritoneum of mice does not involve vanilloid receptors.

More recently, it has been suggested that nuclear receptor family of peroxisome proliferator-activated receptors (PPARs) represent the additional nuclear branch of the cannabinoid receptor family (37, 38). CBD has been shown to activate and function via the nuclear receptor, PPAR γ (18, 25, 38, 39). We used pre-administration of selective and potent PPAR γ inhibitor (BADGE) to assess its role in our model. Remarkably, pre-injection with BADGE almost completely blocked the induction of MDSC by CBD *in vivo* (Fig. 10C, D)

which suggested the crucial role of PPAR γ in this pathway. We also treated normal murine cloned mast cells (MC/9) in culture with CBD. MC/9 mast cells showed increased production of G-CSF in response to CBD *in vitro* (Fig. 10E). In some wells PPAR γ was blocked by adding equimolar concentration of BADGE. Blocking of PPAR γ significantly inhibited the G-CSF production induced by CBD in these mast cell cultures.

Luc reporter assay: CBD activates PPAR γ

First, we checked for the expression of PPAR γ in mast cells. Both murine cloned mast cells (MC/9) and P819 mast cell line showed significant expression of PPAR γ mRNA in RT-PCR analysis (Fig. 11A). To test whether CBD can induce PPAR γ transcriptional activity, we used PPAR-luciferase reporter system (Fig. 11B). P815 cells were transfected with the PPAR-luciferase reporter construct followed by treatment with CBD. Luciferase activity was determined by dual luciferase bioluminescence assay system. Inducible PPAR-responsive firefly luciferase reporter activity was normalized to co-transfected constitutive Renilla-luciferase used as the internal control to account for transfection variations. CBD significantly induced the transcriptional reporter activity similar to troglitazone, a known PPAR γ agonist (Fig. 11C), suggesting that CBD can directly activate PPAR γ .

DISCUSSION

MDSC are non-terminally differentiated, immature myeloid cells that have acquired a highly immunosuppressive functional phenotype. These cells are of great interest in cancer as well as inflammation as they potently suppress the cytotoxic activities of natural killer and natural killer T cells, and immune responses mediated by CD4 and CD8 T cells (40, 41). Under normal conditions, precursor myeloid cells from bone marrow differentiate into mature granulocytes, macrophages or dendritic cells as they home to peripheral organs. However, various mediators produced during pathological conditions such as cancer, infections, trauma, autoimmunity, and sometimes in response to certain natural compounds, are believed to cause the proliferation of immature myeloid cells while blocking their terminal differentiation resulting in the accumulation of immunosuppressive MDSC phenotype (42). Recent studies from our laboratory have explored the induction MDSC as an important mechanism action of several natural compounds with known immunosuppressive or anti-inflammatory properties including marijuana cannabinoids and resveratrol (27, 28, 43–45). The potent immunomodulatory action of CBD is known and its effect on the activated immune system has been the subject of a number of studies (5, 16–23, 27, 39, 46–49). However, our understanding of the effects and underlying mechanisms of CBD exposure on naïve immune system is limited. In the current study, we provide evidence that CBD can induce a large number of MDSC *in vivo* in normal mice. This was found to be associated with enhanced levels of chemokines G-CSF, CXCL-1 (KC) and M-CSF but not GM-CSF. Furthermore, blocking of G-CSF *in vivo* using anti-G-CSF antibody was able to significantly inhibit the accumulation of MDSC in response to CBD. CBD-induced MDSC demonstrated potent immunosuppressive activity by suppressing T cell proliferation *ex vivo* as well as upon adoptive transfer *in vivo* in LPS-induced, acute inflammatory response.

Pathways identified in cancer or inflammation where suppressive MDSCs have been demonstrated to be induced in response to tumor derived factors or inflammatory mediators, respectively (15, 50, 51). The *in vivo* response to CBD appears to be unlike a typical inflammatory response. Our studies have identified a third pathway wherein immunosuppressive natural compounds such as cannabinoids trigger specific chemokine milieu even in a naïve system resulting in the accumulation and activation of predominantly functional MDSC response in the periphery primarily derived from BM myeloid precursors. These data are consistent with a number of immunosuppressive compounds that induce MDSCs following activation of AhR, cannabinoid receptors or vanilloid receptors and the like (27, 28, 45).

Multiple pathways have been shown to be responsible for MDSC-mediated T cell suppression (11, 12, 41, 52). Production of Arg1 enzyme appears to be one of the most crucial mechanisms as both granulocytic and monocytic subsets of MDSC are known to express Arg1. Arg1 acts by metabolizing L-arginine, an essential amino acid needed for T cell proliferation and survival, thus inhibiting T cell proliferation. We observed that CBD-induced MDSC expressed functional Arg1. In addition, T cell suppressive activity of CBD-induced MDSC was significantly attenuated in the presence of a specific arginase inhibitor.

Although, a partial or weak agonist for the vanilloid receptors (EC₅₀, 3.5 μM), CBD has been shown to function by activating Trpv1 in several models of inflammation (19, 53). In this study, using Trpv1^{-/-} mice we have observed that induction of MDSC by CBD in the naïve peritoneum was completely independent of Trpv1. This is particularly interesting because anti-inflammatory effect of CBD in experimental hepatitis was Trpv1-dependent and was associated with increased MDSC numbers in liver (27). This suggests that unlike local, robust MDSC response to CBD in the peritoneum in naïve mice, migration and accumulation of MDSC in other organs, especially during active inflammatory response may involve Trpv1-dependent mechanisms. Additionally, different mechanisms may come into play in activated versus normal conditions, and Trpv1 may have different roles during inflammation as opposed to naïve system. Further, peritoneum being recognized as a unique immune organ, it is likely that phenotype of peritoneal mast cells, with respect to expression and/or function of PPARγ, release chemokine mediators such as G-CSF and their involvement in the induction of MDSC in response to CBD may be organ-specific. It is well known that CBD has a complex pharmacology (1) and functions by binding and activating different receptors in different models. Some *in vivo* effects of cannabidiol have been previously attributed to CB1 (26, 54–56) and CB2 receptors (55, 57, 58), although the general agreement in the field is that CBD exhibits little affinity towards these cannabinoid receptors. Recently, CBD has been shown to function by binding to adenosine receptor A_{2A} (46, 48, 57). Neuroprotective effect of CBD in hypoxic-ischemic brain damage (57), anti-inflammatory effect in retina (48) and acute lung injury (46) have been shown to involve A_{2A} receptors. We studied the possible involvement of these receptors initially in the current study by pre-injecting CB1/ CB2 antagonists or specific A_{2A} inhibitor. We did not see any effect of these inhibitors on the induction of MDSC by CBD *in vivo* (data not shown).

Our results using PPARγ inhibitor *in vivo* clearly demonstrated the critical role of this nuclear receptor-transcription factor in the induction of MDSC by CBD. Others have

previously demonstrated PPAR γ agonist activity of CBD in several models (18, 24, 25, 39, 59). CBD was shown to increase the transcriptional activity of PPAR γ and modulate cellular functions in rat aortic cells and fibroblasts (25). Recent studies have shown that CBD can reduce intestinal inflammation as well as β -amyloid-induced neuroinflammation acting selectively via PPAR γ pathway (18, 39). We observed that the induction of MDSC by CBD was almost entirely mediated by PPAR γ as pretreatment with potent PPAR γ antagonist BADGE was able to completely inhibit the response. Further, PPAR γ antagonist was able to block the production of G-CSF *in vivo* in the peritoneum, and by normal mouse MC/9 mast cells *in vitro* in response to CBD. Based on luciferase reporter assay, we further showed that CBD directly activated PPAR γ . These results suggest that CBD may induce the production of G-CSF and other chemokine mediators such as CXCL1 and M-CSF by activating PPAR γ receptor *in vivo* which may promote the differentiation, migration and proliferation of MDSC from bone marrow precursors.

Our experiments using c-Kit mutant Kit^{W/W-v} that are also deficient in mast cells showed that induction of G-CSF and MDSC by CBD was significantly attenuated in these mice suggesting the crucial role of c-Kit. The restoration of response following adoptive transfer of mast cells indicated the likely role of mast cells and that mast cells might be the crucial responders in this pathway. This was further supported by the fact that a well known mast cell activator compound was able to induce MDSC cellular response in the peritoneum similar to CBD *in vivo*. Role of mast cells in the mobilization and function of MDSC has been previously demonstrated using *in vivo* tumor-models (60, 61). Nevertheless, given the fact that c-Kit is crucial for hematopoiesis and MDSC generation, and further reconstitution with BM-derived mast cells in these mice only replenishes mast cells on a c-kit-deficient background, the role of mast cells needs to be ultimately confirmed using new *Cre* transgenic model systems (62) devoid of defects in c-Kit or its ligand stem cell factor.

PPARs are group of nuclear hormone receptor superfamily of transcription factors that are triggered by hormones, endogenous fatty acids, and by various nutritional or natural compounds (63). Activated PPARs bind to specific regions of DNA termed peroxisome proliferator hormone response elements to promote or prevent transcription of specific genes. Activated PPARs are capable of functioning by DNA-independent mechanism of protein-protein interactions with other transcription factors to cause transcriptional repression (64). Two classes of PPAR agonists, namely, fibrates (PPAR α agonist) and thiazolidinediones (PPAR γ agonist) have been approved by US FDA for pharmaceutical use. Clinically, PPAR γ activating drugs have been used in the treatment of dyslipidemia and insulin insensitivity in type II diabetes (65), and have shown potential in degrading β -amyloid plaques in Alzheimer's disease (66). In addition to being a key regulator in lipogenesis and adipocyte differentiation, PPAR γ may play a role in innate immunity particularly by regulating immune cell differentiation and function (67, 68). Our understanding of the role of PPAR γ in the induction of regulatory immune cells is limited. Recently, the suppressive function of M2-like MDSC was shown to be mediated by arg1 and PPAR γ (69). Bisphenol A diglycidyl ether or BADGE used in this study is a selective antagonist of PPAR γ over PPAR α and PPAR δ (70). This compound has been previously used *in vivo* in effectively reversing the anti-inflammatory effects of PPAR γ agonists (71).

Activation of PPAR γ by CBD may have consequences in cancer and infectious diseases, and therapeutic potential in inflammatory and neurodegenerative disorders. Our results also suggest a potential for the use of PPAR γ selective agonists *in vivo* in the modulation of MDSC mobilization and function.

Marijuana is an illegal drug in many countries including United States. However, several states in US have enacted laws in recent years to legalize medicinal and recreational use of cannabis based on popular initiatives. This could lead to marijuana use becoming more acceptable and its use may increase in coming years. THC and CBD are the major psychoactive and non-psychoactive components of marijuana respectively. Due to the preference for varieties that were more mind-altering with a higher THC levels, selective breeding for decades had lead to *Cannabis* strains with low CBD content (72). However, more CBD-rich strains are being developed in recent years owing to its demand in medical cannabis patients (73). Our previous studies showed significant induction of functional MDSC *in vivo* by THC as well as altered regulation of microRNA and target genes in THC-induced MDSC (28, 74). Because marijuana contains both THC and CBD, together our studies suggest that ingestion of marijuana may lead to potent induction of MDSC.

In conclusion, the major non-psychoactive natural cannabinoid from cannabis, cannabidiol (CBD), caused robust induction of highly immunosuppressive, functional CD11b⁺Gr-1⁺ MDSC *in vivo* in naïve mice. The induction of MDSC was dependent on c-Kit, mast cells and was mediated by transcription factor PPAR γ and chemokine mediators, particularly G-CSF (Fig. 12). These observations enhance our understanding of the effects of CBD on the immune system and clearly establish that induction of MDSC is one of the major mechanisms of action of CBD *in vivo*. While these findings support the development of CBD as a potential anti-inflammatory therapeutic, at the same time they also highlight the importance of more precisely understanding the possible negative consequences of its use in cancer, as immunosuppression caused by MDSC has been shown to play a major role in tumor evasion.

Acknowledgments

This research was supported in whole or part by National Institutes of Health, USA grant awards K01DA034892 (to V.L.H.); P01AT003961, P20RR032684, R01AT006888, R01ES019313, R01MH094755 and VA Merit Award|01BX001357 (to P.S.N and M.N.).

References

1. Pertwee RG. Pharmacology of cannabinoid receptor ligands. *Curr Med Chem.* 1999; 6:635–64. [PubMed: 10469884]
2. Esposito G, De Filippis D, Maiuri MC, De Stefano D, Carnuccio R, Iuvone T. Cannabidiol inhibits inducible nitric oxide synthase protein expression and nitric oxide production in beta-amyloid stimulated PC12 neurons through p38 MAP kinase and NF-kappaB involvement. *Neurosci Lett.* 2006; 399:91–95. [PubMed: 16490313]
3. Hampson AJ, Grimaldi M, Axelrod J, Wink D. Cannabidiol and (-)-Delta9-tetrahydrocannabinol are neuroprotective antioxidants. *Proc Natl Acad Sci USA.* 1998; 95:8268–8273. [PubMed: 9653176]
4. El-Remessy AB, Al-Shabrawey M, Khalifa Y, Tsai N-T, Caldwell RB, Liou GI. Neuroprotective and blood-retinal barrier-preserving effects of cannabidiol in experimental diabetes. *Am J Pathol.* 2006; 168:235–244. [PubMed: 16400026]

5. Esposito G, Scuderi C, Savani C, Steardo L, De Filippis D, Cottone P, Iuvone T, Cuomo V, Steardo L. Cannabidiol in vivo blunts beta-amyloid induced neuroinflammation by suppressing IL-1beta and iNOS expression. *Br J Pharmacol.* 2007; 151:1272–9. [PubMed: 17592514]
6. Booz GW. Cannabidiol as an emergent therapeutic strategy for lessening the impact of inflammation on oxidative stress. *Free Radic Biol Med.* 2011
7. Sastre-Garriga J, Vila C, Clissold S, Montalban X. THC and CBD oromucosal spray (Sativex®) in the management of spasticity associated with multiple sclerosis. *Expert Rev Neurother.* 2011; 11:627–637. [PubMed: 21456949]
8. Perez J. Combined cannabinoid therapy via an oromucosal spray. *Drugs Today.* 2006; 42:495–503. [PubMed: 16969427]
9. Gallina G, Dolcetti L, Serafini P, De Santo C, Marigo I, Colombo MP, Basso G, Brombacher F, Borrello I, Zanovello P, Bicciato S, Bronte V. Tumors induce a subset of inflammatory monocytes with immunosuppressive activity on CD8+ T cells. *J Clin Invest.* 2006; 116:2777–90. [PubMed: 17016559]
10. Serafini P, Borrello I, Bronte V. Myeloid suppressor cells in cancer: recruitment, phenotype, properties, and mechanisms of immune suppression. *Semin Cancer Biol.* 2006; 16:53–65. [PubMed: 16168663]
11. Bronte V, Serafini P, Mazzoni A, Segal DM, Zanovello P. L-arginine metabolism in myeloid cells controls T-lymphocyte functions. *Trends Immunol.* 2003; 24:302–6. [PubMed: 12810105]
12. Gabrilovich DI, Nagaraj S. Myeloid-derived suppressor cells as regulators of the immune system. *Nat Rev Immunol.* 2009; 9:162–74. [PubMed: 19197294]
13. Angulo I, de las Heras FG, García-Bustos JF, Gargallo D, Muñoz-Fernández MA, Fresno M. Nitric oxide-producing CD11b(+)Ly-6G(Gr-1)(+)CD31(ER-MP12)(+) cells in the spleen of cyclophosphamide-treated mice: implications for T-cell responses in immunosuppressed mice. *Blood.* 2000; 95:212–220. [PubMed: 10607705]
14. Haile LA, von Wasielewski R, Gamrekashvili J, Krüger C, Bachmann O, Westendorf AM, Buer J, Liblau R, Manns MP, Korangy F, Greten TF. Myeloid-derived suppressor cells in inflammatory bowel disease: a new immunoregulatory pathway. *Gastroenterology.* 2008; 135:871–881. 881.e1–5. [PubMed: 18674538]
15. Ostrand-Rosenberg S, Sinha P. Myeloid-derived suppressor cells: linking inflammation and cancer. *J Immunol.* 2009; 182:4499–4506. [PubMed: 19342621]
16. Malfait AM, Gallily R, Sumariwalla PF, Malik AS, Andreaskos E, Mechoulam R, Feldmann M. The nonpsychoactive cannabis constituent cannabidiol is an oral anti-arthritis therapeutic in murine collagen-induced arthritis. *Proc Natl Acad Sci USA.* 2000; 97:9561–9566. [PubMed: 10920191]
17. Rajesh M, Mukhopadhyay P, Bátkai S, Haskó G, Liaudet L, Drel VR, Obrosova IG, Pacher P. Cannabidiol attenuates high glucose-induced endothelial cell inflammatory response and barrier disruption. *Am J Physiol Heart Circ Physiol.* 2007; 293:H610–619. [PubMed: 17384130]
18. Esposito G, Scuderi C, Valenza M, Togna GI, Latina V, De Filippis D, Cipriano M, Carratù MR, Iuvone T, Steardo L. Cannabidiol reduces A β -induced neuroinflammation and promotes hippocampal neurogenesis through PPAR γ involvement. *PLoS ONE.* 2011; 6:e28668. [PubMed: 22163051]
19. Costa B, Colleoni M, Conti S, Parolaro D, Franke C, Trovato AE, Giagnoni G. Oral anti-inflammatory activity of cannabidiol, a non-psychoactive constituent of cannabis, in acute carrageenan-induced inflammation in the rat paw. *Naunyn Schmiedebergs Arch Pharmacol.* 2004; 369:294–9. [PubMed: 14963641]
20. Weiss L, Zeira M, Reich S, Slavin S, Raz I, Mechoulam R, Gallily R. Cannabidiol arrests onset of autoimmune diabetes in NOD mice. *Neuropharmacology.* 2008; 54:244–249. [PubMed: 17714746]
21. Durst R, Danenberg H, Gallily R, Mechoulam R, Meir K, Grad E, Beeri R, Pugatsch T, Tarsish E, Lotan C. Cannabidiol, a nonpsychoactive Cannabis constituent, protects against myocardial ischemic reperfusion injury. *Am J Physiol Heart Circ Physiol.* 2007; 293:H3602–7. [PubMed: 17890433]

22. Ruiz-Valdepeñas L, Martínez-Orgado JA, Benito C, Millán A, Tolón RM, Romero J. Cannabidiol reduces lipopolysaccharide-induced vascular changes and inflammation in the mouse brain: an intravital microscopy study. *J Neuroinflammation*. 2011; 8:5. [PubMed: 21244691]
23. Kozela E, Lev N, Kaushansky N, Eilam R, Rimmerman N, Levy R, Ben-Nun A, Juknat A, Vogel Z. Cannabidiol inhibits pathogenic T cells, decreases spinal microglial activation and ameliorates multiple sclerosis-like disease in C57BL/6 mice. *Br J Pharmacol*. 2011; 163:1507–19. [PubMed: 21449980]
24. Ramer R, Heinemann K, Merkord J, Rohde H, Salamon A, Linnebacher M, Hinz B. COX-2 and PPAR- γ confer cannabidiol-induced apoptosis of human lung cancer cells. *Mol Cancer Ther*. 2013; 12:69–82. [PubMed: 23220503]
25. O'Sullivan SE, Sun Y, Bennett AJ, Randall MD, Kendall DA. Time-dependent vascular actions of cannabidiol in the rat aorta. *Eur J Pharmacol*. 2009; 612:61–68. [PubMed: 19285060]
26. Alhamoruni A, Lee AC, Wright KL, Larvin M, O'Sullivan SE. Pharmacological effects of cannabinoids on the Caco-2 cell culture model of intestinal permeability. *J Pharmacol Exp Ther*. 2010; 335:92–102. [PubMed: 20592049]
27. Hegde VL, Nagarkatti PS, Nagarkatti M. Role of myeloid-derived suppressor cells in amelioration of experimental autoimmune hepatitis following activation of TRPV1 receptors by cannabidiol. *PLoS one*. 2011; 6:e18281. [PubMed: 21483776]
28. Hegde VL, Nagarkatti M, Nagarkatti PS. Cannabinoid receptor activation leads to massive mobilization of myeloid-derived suppressor cells with potent immunosuppressive properties. *European journal of immunology*. 2010; 40:3358–71. [PubMed: 21110319]
29. Shelburne CP, McCoy ME, Piekorz R, Sexl V, Roh K-H, Jacobs-Helber SM, Gillespie SR, Bailey DP, Mirmonsef P, Mann MN, Kashyap M, Wright HV, Chong HJ, Bouton LA, Barnstein B, Ramirez CD, Bunting KD, Sawyer S, Lantz CS, Ryan JJ. Stat5 expression is critical for mast cell development and survival. *Blood*. 2003; 102:1290–1297. [PubMed: 12714518]
30. Poltorak A, He X, Smirnova I, Liu M-Y, Huffel CV, Du X, Birdwell D, Alejos E, Silva M, Galanos C, Freudenberg M, Ricciardi-Castagnoli P, Layton B, Beutler B. Defective LPS Signaling in C3H/HeJ and C57BL/10ScCr Mice: Mutations in Tlr4 Gene. *Science*. 1998; 282:2085–2088. [PubMed: 9851930]
31. Hoover-Plow JL, Gong Y, Shchurin A, Busuttill SJ, Schneeman TA, Hart E. Strain and model dependent differences in inflammatory cell recruitment in mice. *Inflamm Res*. 2008; 57:457–463. [PubMed: 18827970]
32. Bronte V, Apolloni E, Cabrelle A, Ronca R, Serafini P, Zamboni P, Restifo NP, Zanovello P. Identification of a CD11b(+)/Gr-1(+)/CD31(+) myeloid progenitor capable of activating or suppressing CD8(+) T cells. *Blood*. 2000; 96:3838–3846. [PubMed: 11090068]
33. Hock H, Hamblen MJ, Rooke HM, Traver D, Bronson RT, Cameron S, Orkin SH. Intrinsic requirement for zinc finger transcription factor Gfi-1 in neutrophil differentiation. *Immunity*. 2003; 18:109–120. [PubMed: 12530980]
34. Dolcetti L, Peranzoni E, Ugel S, Marigo I, Fernandez Gomez A, Mesa C, Geilich M, Winkels G, Traggiai E, Casati A, Grassi F, Bronte V. Hierarchy of immunosuppressive strength among myeloid-derived suppressor cell subsets is determined by GM-CSF. *Eur J Immunol*. 2010; 40:22–35. [PubMed: 19941314]
35. Raychaudhuri B, Rayman P, Ireland J, Ko J, Rini B, Borden EC, Garcia J, Vogelbaum MA, Finke J. Myeloid-derived suppressor cell accumulation and function in patients with newly diagnosed glioblastoma. *Neuro Oncol*. 2011; 13:591–9. [PubMed: 21636707]
36. Costa B, Giagnoni G, Franke C, Trovato AE, Colleoni M. Vanilloid TRPV1 receptor mediates the antihyperalgesic effect of the nonpsychoactive cannabinoid, cannabidiol, in a rat model of acute inflammation. *Br J Pharmacol*. 2004; 143:247–50. [PubMed: 15313881]
37. Pertwee RG, Howlett AC, Abood ME, Alexander SPH, Di Marzo V, Elphick MR, Greasley PJ, Hansen HS, Kunos G, Mackie K, Mechoulam R, Ross RA. International Union of Basic and Clinical Pharmacology. LXXIX. Cannabinoid receptors and their ligands: beyond CB and CB₂. *Pharmacol Rev*. 2010; 62:588–631. [PubMed: 21079038]

38. O'Sullivan SE, Kendall DA. Cannabinoid activation of peroxisome proliferator-activated receptors: potential for modulation of inflammatory disease. *Immunobiology*. 2010; 215:611–6. [PubMed: 19833407]
39. De, Filippis D.; Esposito, G.; Cirillo, C.; Cipriano, M.; De Winter, BY.; Scuderi, C.; Sarnelli, G.; Cuomo, R.; Steardo, L.; De Man, JG.; Iuvone, T. Cannabidiol reduces intestinal inflammation through the control of neuroimmune axis. *PLoS ONE*. 2011; 6:e28159. [PubMed: 22163000]
40. Dolcetti L, Marigo I, Mantelli B, Peranzoni E, Zanollo P, Bronte V. Myeloid-derived suppressor cell role in tumor-related inflammation. *Cancer Lett*. 2008; 267:216–25. [PubMed: 18433992]
41. Ostrand-Rosenberg S. Myeloid-derived suppressor cells: more mechanisms for inhibiting antitumor immunity. *Cancer Immunol Immunother*. 2010; 59:1593–600. [PubMed: 20414655]
42. Bronte V. Myeloid-derived suppressor cells in inflammation: uncovering cell subsets with enhanced immunosuppressive functions. *Eur J Immunol*. 2009; 39:2670–2. [PubMed: 19757440]
43. Singh UP, Singh NP, Singh B, Hofseth LJ, Taub DD, Price RL, Nagarkatti M, Nagarkatti PS. Role of resveratrol-induced CD11b(+) Gr-1(+) myeloid derived suppressor cells (MDSCs) in the reduction of CXCR3(+) T cells and amelioration of chronic colitis in IL-10(–/–) mice. *Brain Behav Immun*. 2012; 26:72–82. [PubMed: 21807089]
44. Rieder SA, Nagarkatti P, Nagarkatti M. Multiple anti-inflammatory pathways triggered by resveratrol lead to amelioration of staphylococcal enterotoxin B-induced lung injury. *Br J Pharmacol*. 2012; 167:1244–1258. [PubMed: 22646800]
45. Guan H, Singh NP, Singh UP, Nagarkatti PS, Nagarkatti M. Resveratrol prevents endothelial cells injury in high-dose interleukin-2 therapy against melanoma. *PLoS ONE*. 2012; 7:e35650. [PubMed: 22532866]
46. Ribeiro A, Ferraz-de-Paula V, Pinheiro ML, Vitoretti LB, Mariano-Souza DP, Quinteiro-Filho WM, Akamine AT, Almeida VI, Quevedo J, Dal-Pizzol F, Hallak JE, Zuardi AW, Crippa JA, Palermo-Neto J. Cannabidiol, a non-psychoactive plant-derived cannabinoid, decreases inflammation in a murine model of acute lung injury: role for the adenosine A(2A) receptor. *Eur J Pharmacol*. 2012; 678:78–85. [PubMed: 22265864]
47. Li K, Feng J-Y, Li Y-Y, Yuece B, Lin X-H, Yu L-Y, Li Y-N, Feng Y-J, Storr M. Anti-Inflammatory Role of Cannabidiol and O-1602 in Cerulein-Induced Acute Pancreatitis in Mice. *Pancreas*. 2012
48. Liou GI, Auchampach JA, Hillard CJ, Zhu G, Yousufzai B, Mian S, Khan S, Khalifa Y. Mediation of cannabidiol anti-inflammation in the retina by equilibrative nucleoside transporter and A2A adenosine receptor. *Invest Ophthalmol Vis Sci*. 2008; 49:5526–31. [PubMed: 18641283]
49. Jan TR, Su ST, Wu HY, Liao MH. Suppressive effects of cannabidiol on antigen-specific antibody production and functional activity of splenocytes in ovalbumin-sensitized BALB/c mice. *Int Immunopharmacol*. 2007; 7:773–80. [PubMed: 17466911]
50. Sade-Feldman M, Kanterman J, Ish-Shalom E, Elnekave M, Horwitz E, Baniyash M. Tumor necrosis factor- α blocks differentiation and enhances suppressive activity of immature myeloid cells during chronic inflammation. *Immunity*. 2013; 38:541–554. [PubMed: 23477736]
51. Sinha P, Okoro C, Foell D, Freeze HH, Ostrand-Rosenberg S, Srikrishna G. Proinflammatory S100 proteins regulate the accumulation of myeloid-derived suppressor cells. *J Immunol*. 2008; 181:4666–4675. [PubMed: 18802069]
52. Srivastava MK, Sinha P, Clements VK, Rodriguez P, Ostrand-Rosenberg S. Myeloid-derived suppressor cells inhibit T-cell activation by depleting cystine and cysteine. *Cancer Res*. 2010; 70:68–77. [PubMed: 20028852]
53. Costa B, Trovato AE, Comelli F, Giagnoni G, Colleoni M. The non-psychoactive cannabis constituent cannabidiol is an orally effective therapeutic agent in rat chronic inflammatory and neuropathic pain. *Eur J Pharmacol*. 2007; 556:75–83. [PubMed: 17157290]
54. Fride E, Ponde D, Breuer A, Hanus L. Peripheral, but not central effects of cannabidiol derivatives: mediation by CB(1) and unidentified receptors. *Neuropharmacology*. 2005; 48:1117–29. [PubMed: 15910887]
55. Thomas A, Baillie GL, Phillips AM, Razdan RK, Ross RA, Pertwee RG. Cannabidiol displays unexpectedly high potency as an antagonist of CB1 and CB2 receptor agonists in vitro. *Br J Pharmacol*. 2007; 150:613–23. [PubMed: 17245363]

56. Capasso R, Borrelli F, Aviello G, Romano B, Scalisi C, Capasso F, Izzo AA. Cannabidiol, extracted from *Cannabis sativa*, selectively inhibits inflammatory hypermotility in mice. *Br J Pharmacol*. 2008; 154:1001–8. [PubMed: 18469842]
57. Castillo A, Tolon MR, Fernandez-Ruiz J, Romero J, Martinez-Orgado J. The neuroprotective effect of cannabidiol in an in vitro model of newborn hypoxic-ischemic brain damage in mice is mediated by CB(2) and adenosine receptors. *Neurobiol Dis*. 2010; 37:434–40. [PubMed: 19900555]
58. Kaplan BLF, Springs AEB, Kaminski NE. The profile of immune modulation by cannabidiol (CBD) involves deregulation of nuclear factor of activated T cells (NFAT). *Biochem Pharmacol*. 2008; 76:726–737. [PubMed: 18656454]
59. Burstein S. PPAR-gamma: a nuclear receptor with affinity for cannabinoids. *Life Sci*. 2005; 77:1674–1684. [PubMed: 16005906]
60. Saleem SJ, Martin RK, Morales JK, Sturgill JL, Gibb DR, Graham L, Bear HD, Manjili MH, Ryan JJ, Conrad DH. Cutting edge: mast cells critically augment myeloid-derived suppressor cell activity. *J Immunol*. 2012; 189:511–515. [PubMed: 22706087]
61. Yang Z, Zhang B, Li D, Lv M, Huang C, Shen G-X, Huang B. Mast cells mobilize myeloid-derived suppressor cells and Treg cells in tumor microenvironment via IL-17 pathway in murine hepatocarcinoma model. *PLoS ONE*. 2010; 5:e8922. [PubMed: 20111717]
62. Lilla JN, Chen C-C, Mukai K, BenBarak MJ, Franco CB, Kalesnikoff J, Yu M, Tsai M, Piliponsky AM, Galli SJ. Reduced mast cell and basophil numbers and function in Cpa3-Cre; Mcl-1fl/fl mice. *Blood*. 2011; 118:6930–6938. [PubMed: 22001390]
63. Berger J, Moller DE. The mechanisms of action of PPARs. *Annu Rev Med*. 2002; 53:409–435. [PubMed: 11818483]
64. Oliveira ACP, Bertollo CM, Rocha LTS, Nascimento EB Jr, Costa KA, Coelho MM. Antinociceptive and anti-inflammatory activities of fenofibrate, an agonist of PPAR alpha, and pioglitazone, an agonist of PPAR gamma. *Eur J Pharmacol*. 2007; 561:194–201. [PubMed: 17343847]
65. Ahmadian M, Suh JM, Hah N, Liddle C, Atkins AR, Downes M, Evans RM. PPAR γ signaling and metabolism: the good, the bad and the future. *Nat Med*. 2013; 19:557–566. [PubMed: 23652116]
66. Sato T, Hanyu H, Hirao K, Kanetaka H, Sakurai H, Iwamoto T. Efficacy of PPAR- γ agonist pioglitazone in mild Alzheimer disease. *Neurobiol Aging*. 2011; 32:1626–1633. [PubMed: 19923038]
67. Yasugi E, Horiuchi A, Uemura I, Okuma E, Nakatsu M, Saeki K, Kamisaka Y, Kagechika H, Yasuda K, Yuo A. Peroxisome proliferator-activated receptor gamma ligands stimulate myeloid differentiation and lipogenesis in human leukemia NB4 cells. *Dev Growth Differ*. 2006; 48:177–188. [PubMed: 16573735]
68. Sztatmari I, Rajnavolgyi E, Nagy L. PPARgamma, a lipid-activated transcription factor as a regulator of dendritic cell function. *Ann N Y Acad Sci*. 2006; 1088:207–218. [PubMed: 17192567]
69. Brys L, Beschin A, Raes G, Ghassabeh GH, Noël W, Brandt J, Brombacher F, Baetselier PD. Reactive Oxygen Species and 12/15-Lipoxygenase Contribute to the Antiproliferative Capacity of Alternatively Activated Myeloid Cells Elicited during Helminth Infection. *J Immunol*. 2005; 174:6095–6104. [PubMed: 15879104]
70. Wright HM, Clish CB, Mikami T, Hauser S, Yanagi K, Hiramatsu R, Serhan CN, Spiegelman BM. A synthetic antagonist for the peroxisome proliferator-activated receptor gamma inhibits adipocyte differentiation. *J Biol Chem*. 2000; 275:1873–1877. [PubMed: 10636887]
71. Cuzzocrea S, Pisano B, Dugo L, Ianaro A, Maffia P, Patel NSA, Di Paola R, Ialenti A, Genovese T, Chatterjee PK, Di Rosa M, Caputi AP, Thiemermann C. Rosiglitazone, a ligand of the peroxisome proliferator-activated receptor-gamma, reduces acute inflammation. *Eur J Pharmacol*. 2004; 483:79–93. [PubMed: 14709329]
72. ElSohly, MA. *Marijuana and the Cannabinoids*. Springer Science & Business Media; 2007.
73. Lee, MA. *Smoke Signals: A Social History of Marijuana - Medical, Recreational and Scientific*. Simon and Schuster; 2013.

74. Hegde VL, Tomar S, Jackson A, Rao R, Yang X, Singh UP, Singh NP, Nagarkatti PS, Nagarkatti M. Distinct MicroRNA Expression Profile and Targeted Biological Pathways in Functional Myeloid-derived Suppressor Cells Induced by Δ^9 -Tetrahydrocannabinol in Vivo REGULATION OF CCAAT/ENHANCER-BINDING PROTEIN α BY MicroRNA-690. *Journal of Biological Chemistry*. 2013; 288:36810–36826. [PubMed: 24202177]

Author Manuscript

Author Manuscript

Author Manuscript

Author Manuscript

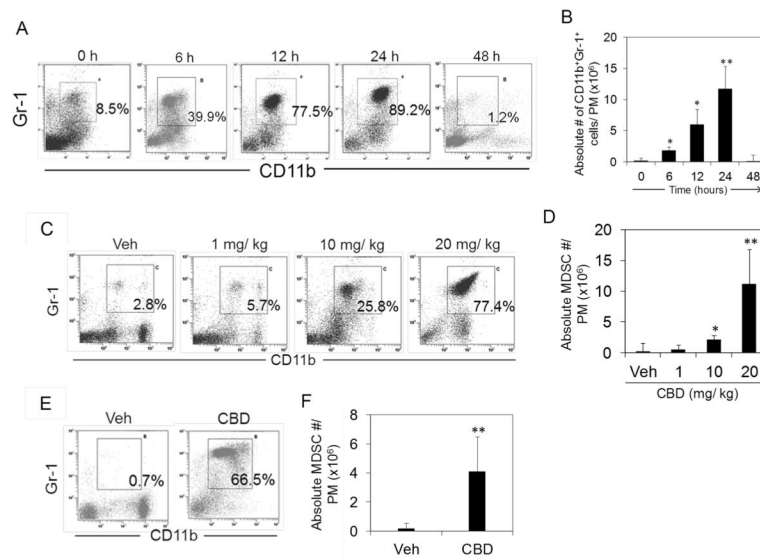


Figure 1. Induction of CD11b⁺Gr-1⁺ cells in response to CBD *in vivo*

A) Time-course of CD11b⁺Gr-1⁺ cell accumulation in WT peritoneum following CBD (20 mg/kg, i.p.) administration. Representative dot plots from FACS analysis are shown for the time points as indicated. B) Absolute number of MDSC calculated from frequency of CD11b⁺Gr-1⁺ cells and total viable cells in each peritoneum, mean \pm SD (n=4). C) Representative dot plots from FACS analysis of cells harvested from peritonea of WT mice (n=4) 16 h after injecting with various doses of CBD as indicated showing dose-dependent induction of CD11b⁺Gr-1⁺ double positive cells. D) Mean \pm SD of absolute MDSC numbers from n=4 mice per group. E, F) Induction of CD11b⁺Gr-1⁺ cells by CBD is independent of TLR4. TLR4-mutant C3H/HeJ mice (n=4) injected with vehicle or 20 mg/kg CBD (i.p.). After 12 h peritoneal exudate cells were analyzed by FACS. Error bars indicate SD. Student's *t*-test: **P*<0.05, ***P*<0.01 compared vs control.

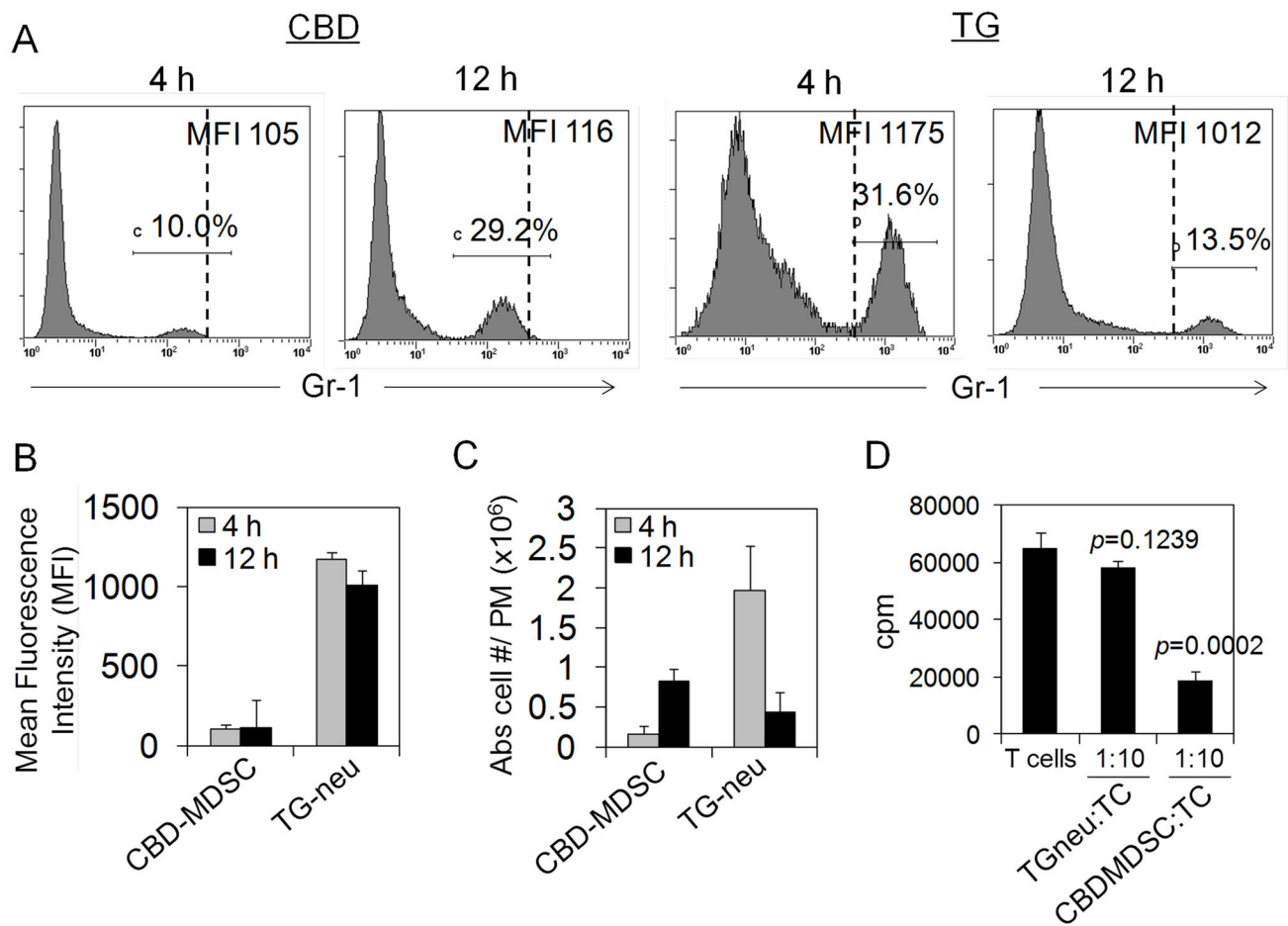


Figure 2. Comparison of in vivo cellular response to CBD and thioglycollate (TG)

WT mice (n=3) were injected (i.p.) with CBD (10 mg/kg) or 0.5 mL of 3% TG. Peritoneal exudate cells were harvested at 4 h or 12 h post-injection and analyzed side-by-side by FACS for Gr-1 (Ly6-G) expression with same voltage settings. Representative histograms are shown (A). B) Mean fluorescence intensities (MFI) for Gr-1 expression. C) Absolute cell numbers per PM for CBD-MDSC (Gr-1^{int}) and TG-neutrophils (Gr1^{high}). D) Syngenic lymph node-derived T cells were stimulated with ConA and co-cultured without or with enriched Gr-1⁺ cells. Data represent mean \pm SD from 3 mice (B, C) or from triplicate determinations (D).

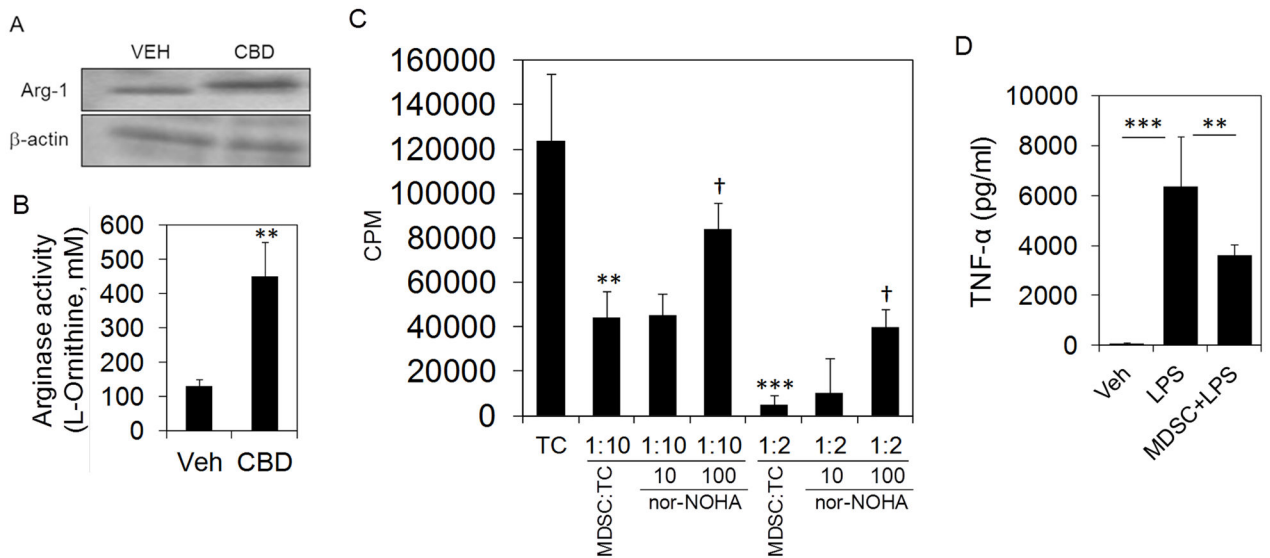


Figure 3. Functional characterization of CD11b⁺Gr-1⁺ cells induced by CBD

Expression of functional Arginase: A) Western blot analysis of lysates of cells harvested from the peritonea, 16 h following the administration of vehicle or 20 mg/kg CBD (n=4); B) Spectrophotometric assay for arginase activity. Cell lysates were analyzed for arginase activity using L-arginine as the substrate, and detecting the L-ornithine formed. Data represent mean \pm SD. Student's *t*-test, ***P*<0.01. C) T cell suppression assay in vitro. CD11b⁺Gr-1⁺ cells harvested from the peritoneum of WT mice were purified to >90% purity, irradiated, plated at 1:10 and 1:2 (MDSC:T cell) ratios with syngenic T cells (2×10^5 T cells/ well) and stimulated with ConA. T cells cultured without MDSC but stimulated with ConA served as control (TC). Arginase inhibitor (nor-NOHA) was added to some wells at 10 or 100 μ M as indicated. Proliferation was assessed at 72 h by [³H]thymidine assay. Data is mean \pm SD of quadruplicate determinations and representative of two experiments. Student's *t*-test: ***P*<0.01, ****P*<0.001 compared to TC control; \dagger *P*<0.05 compared vs corresponding MDSC:TC without nor-NOHA. D) Suppression of acute inflammatory response to LPS in vivo. Purified CBD-induced CD11b⁺Gr-1⁺ cells (5×10^6 / mouse) were adoptively transferred into naïve WT mice two hours before injecting with LPS. One hour after LPS challenge, TNF- α levels in sera were analyzed by ELISA. Data represent mean \pm SD (n=3 mice); Student's *t*-test: ****P*<0.001, ***P*<0.01.

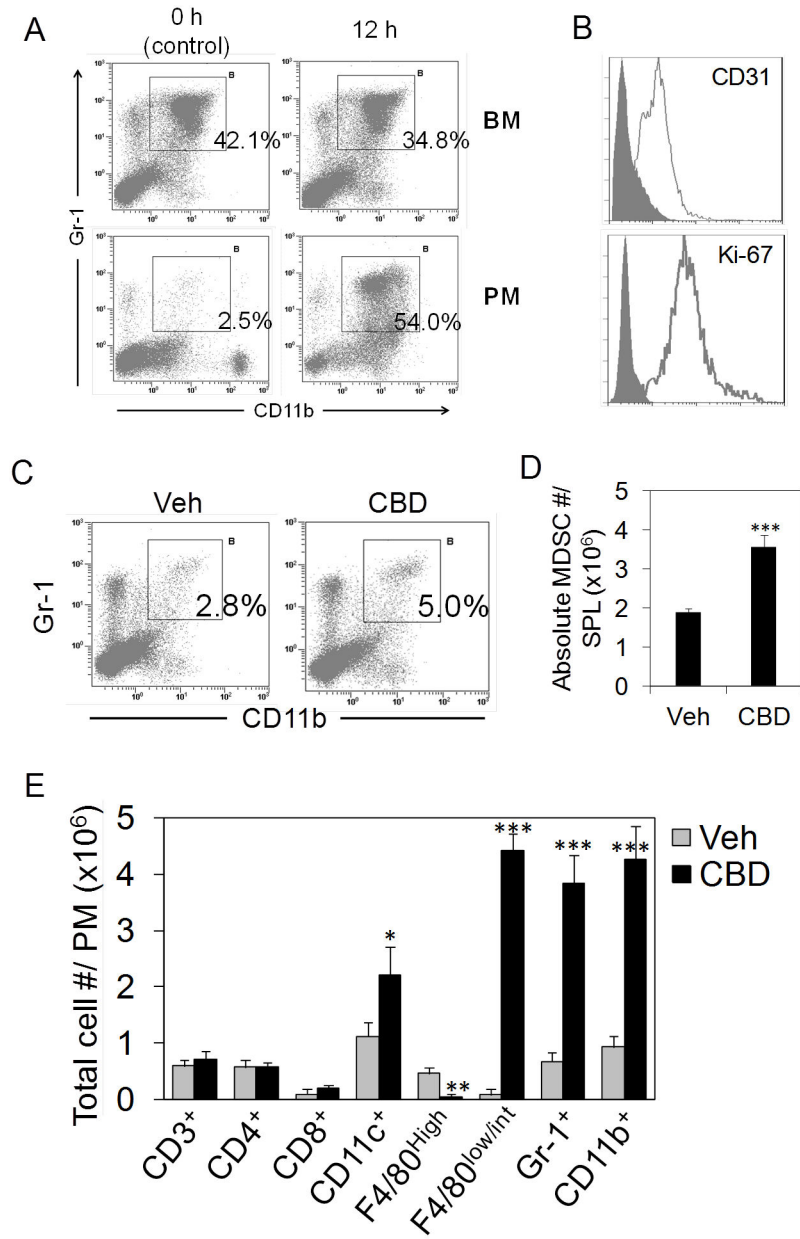


Figure 4.

A) CBD induces mobilization of CD11b⁺Gr-1⁺ MDSCs from BM. Representative dot plots of peritoneal and bone marrow cells harvested 0 or 12 h after CBD (20 mg/kg) administration showing frequency (%) CD11b⁺Gr-1⁺ cells (gated). **B)** Peritoneal cells from CBD injected mice harvested after 12 h were analyzed for CD31 and Ki-67 expression on MDSCs by triple staining along with CD11b and Gr-1. Histograms show expression of CD31 and Ki-67 on gated CD11b⁺Gr-1⁺ MDSC population (open histograms). Filled histograms represent isotype Ab staining controls. **C) Phenotypic analysis for the expression of other markers in peritoneal cells induced by CBD.** Peritoneal cells harvested after 12 h from vehicle or CBD (20 mg/kg) injected mice were stained for indicated markers and analyzed by FACS. The frequency (%) of positive population is

indicated. D, E) Spleen cells harvested after 12 h following vehicle or CBD administration were analyzed for CD11b⁺Gr-1⁺ MDSC by FACS. Representative dot plots showing frequency and mean absolute MDSC numbers (n=3 mice) shown. Error bars indicate SD. *** $P < 0.001$, ** $P < 0.01$, * $P < 0.05$ based on Student's t test (CBD vs Veh control).

Author Manuscript

Author Manuscript

Author Manuscript

Author Manuscript

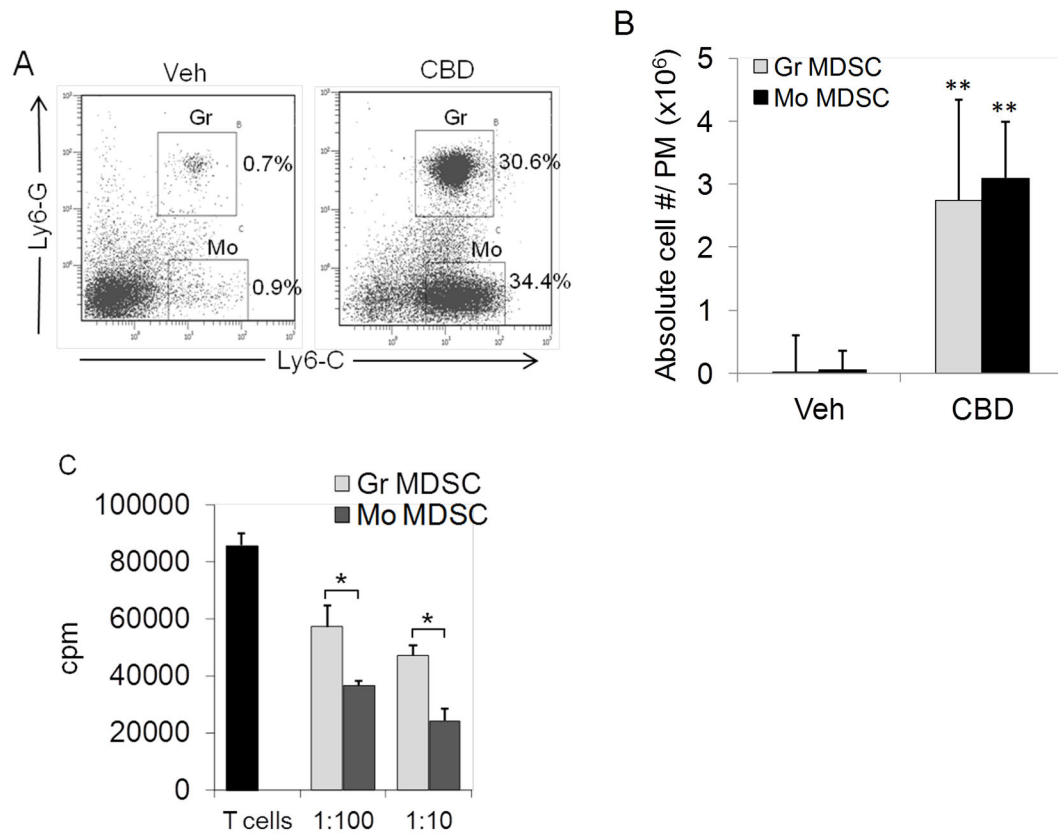


Figure 5. Analysis of CBD-induced MDSC subtypes

WT mice (n=4) were injected with vehicle or 20 mg/kg CBD and after 16 h peritoneal exudate cells were triple-stained for CD11b, Ly6-G and Ly6-C and analyzed by FACS. Representative dot plots with gated CD11b⁺Ly6-G⁺Ly6-C^{+(int)} granulocytic (Gr) and CD11b⁺Ly6-G^{-(neg)}Ly6-C⁺ monocytic (Mo) MDSC subtypes are shown with frequencies indicated (A). Absolute numbers of each sub type is calculated based on frequency and total cell numbers and represented as mean \pm SD from 4 mice (B). Student's *t* test, ***P*<0.01 compared to vehicle control. C) MDSC sub types were purified by FACS sorting and used in T cell suppression assay at indicated ratios with syngenic T cells stimulated with ConA. T cell proliferation was assessed at 72 h by [³H]thymidine incorporation. Mean \pm SD of quadruplicate determinations and representative of two separate experiments shown. **P*<0.05, Student's *t* test.

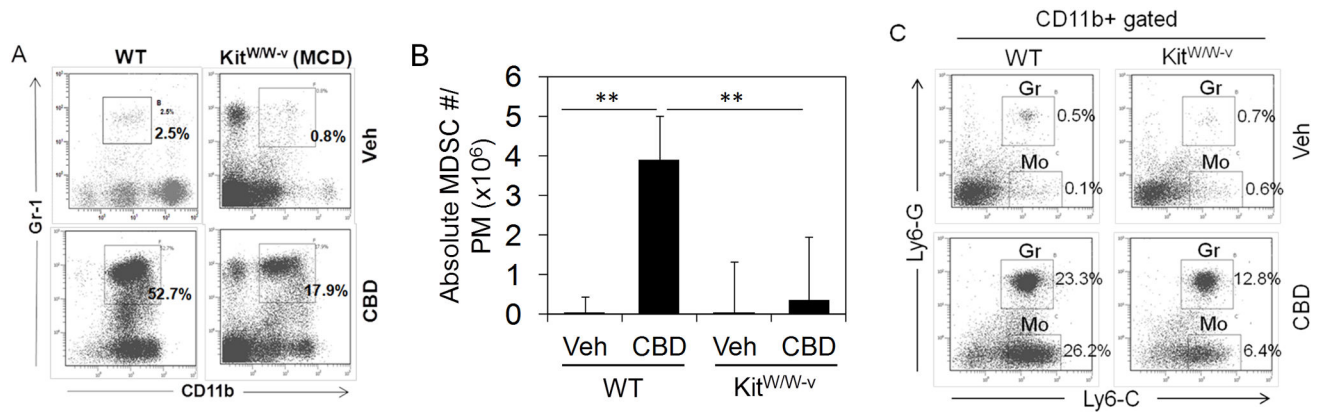


Figure 6. Attenuated induction of MDSC in mast cell-deficient mice

FACS analysis of CD11b⁺Gr-1⁺ MDSC from peritoneum 12 h after injecting with vehicle or CBD in WT or mast cell-deficient Kit^{W/W-v} mice (n=3). Representative dot plots are shown (A). Absolute MDSC cell number is represented as mean ± SD from 3 mice (B). ***P*<0.01, Student's *t* test. C) Cells were analyzed for MDSC subtypes by flow cytometry and frequency of each subset, namely CD11b⁺Ly6-G⁺Ly6-C^(int) granulocytic (Gr) and CD11b⁺Ly6-G^(neg)Ly6-C⁺ monocytic (Mo) MDSC are shown.

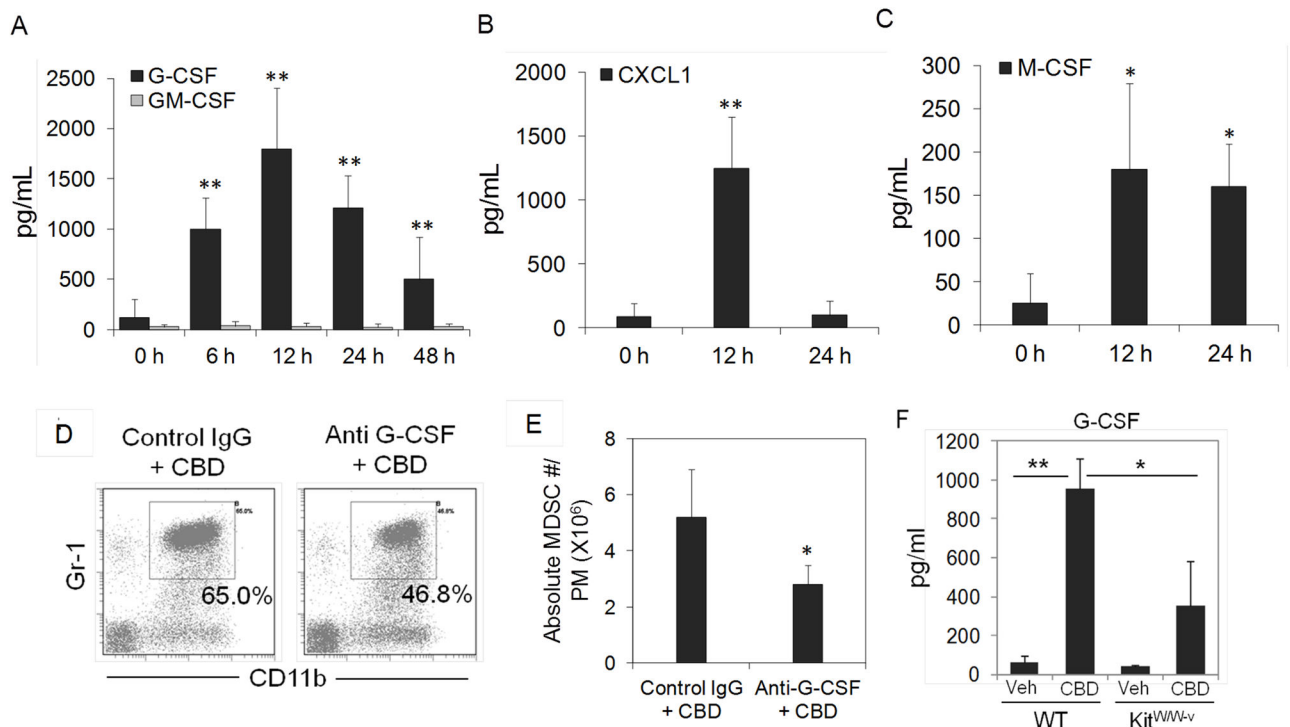


Figure 7. Analysis of chemokines

CBD (20 mg/kg) was injected i.p. into groups of WT mice (n=4) for each time point. G-CSF, GM-CSF, CXCL1 and M-CSF levels in the peritoneal exudates were analyzed by ELISA (A-C). Blocking experiment with anti-G-CSF in vivo: WT mice (n=3) were injected with isotype control IgG or anti-G-CSF Ab (10 μ g/mouse) 1 h before injecting with CBD (20mg/kg). Peritoneal exudate cells were harvested after 12 h, and analyzed by FACS for MDSC. Representative dot plots are shown for each treatment (D); Absolute number of MDSC per peritoneum (n=3 mice) (E). F) G-CSF levels determined by ELISA in the peritoneal exudates of WT and mast cell deficient Kit^{W/W-v} mice 16 h after injection with 20 mg/kg CBD. Error bars indicate SD. Student's *t*-tests: ***P*<0.01, **P*<0.05.

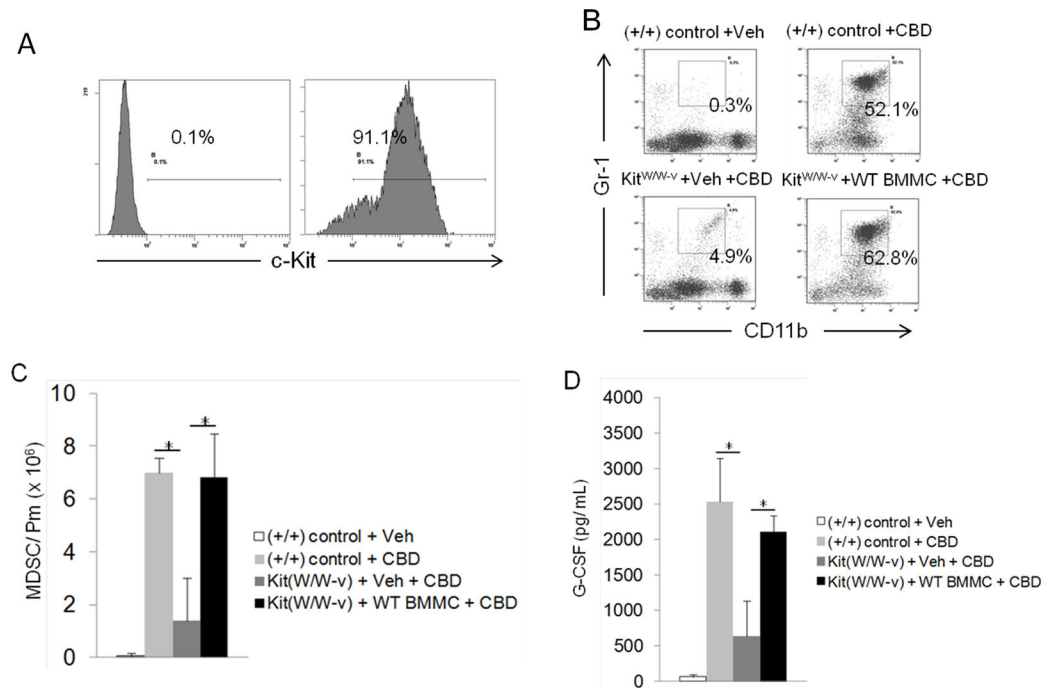


Figure 8. Adoptive transfer of WT mast cells restores CBD response in mast-cell deficient mice
 Bone marrow-derived mast cells (BMMC) were generated by culturing WT bone marrow cells in the presence of recombinant mouse IL-3 and stem cell factor as described in methods. Purity of BMMC after 5 weeks of culture as determined by FACS analysis for c-Kit expression (A); Left histogram isotype control IgG, right histogram c-Kit Ab. BMMC (6×10^6) were adoptively transferred *i.v.* into mast cell-deficient Kit^{W/W-v} mice. Littermates (+/+) were used as WT controls. Mast cells were allowed to engraft and six weeks after transfer, mice with or without adoptively transferred mast cells were injected with vehicle or CBD (*i.p.*). After 16 h, peritoneal exudate cells were analyzed by flow cytometry (B, C). Peritoneal lavage fluids were analyzed for G-CSF by ELISA (D). Data represent mean \pm SD ($n=3$ mice per group). Student's *t*-test: * $P < 0.05$. Successful engraftment of adoptively transferred mast cells was determined by Giemsa staining (Table I).

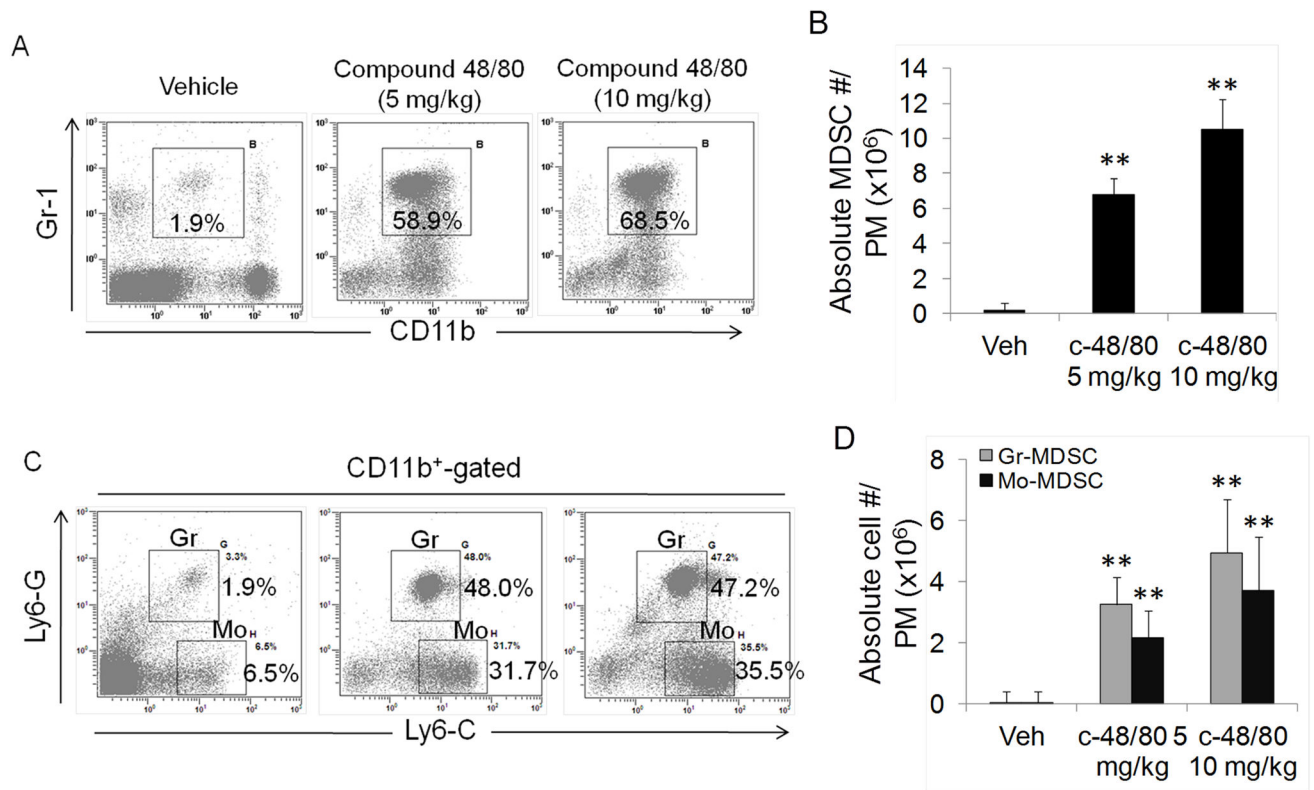


Figure 9. Accumulation of MDSC in response to compound-48/80

WT mice (n=4) were injected with vehicle or different doses of c-48/80 i.p. and peritoneal exudate cells were analyzed by flow cytometry for MDSC. Representative dot plots with frequency of gated CD11b⁺Gr-1⁺ MDSC are shown (A). Absolute MDSC numbers from 4 mice are represented as mean \pm SD (B). C, D) Flow cytometric analysis for MDSC subtypes as described before. Student's *t* test, ***P*<0.01 compared to vehicle control.

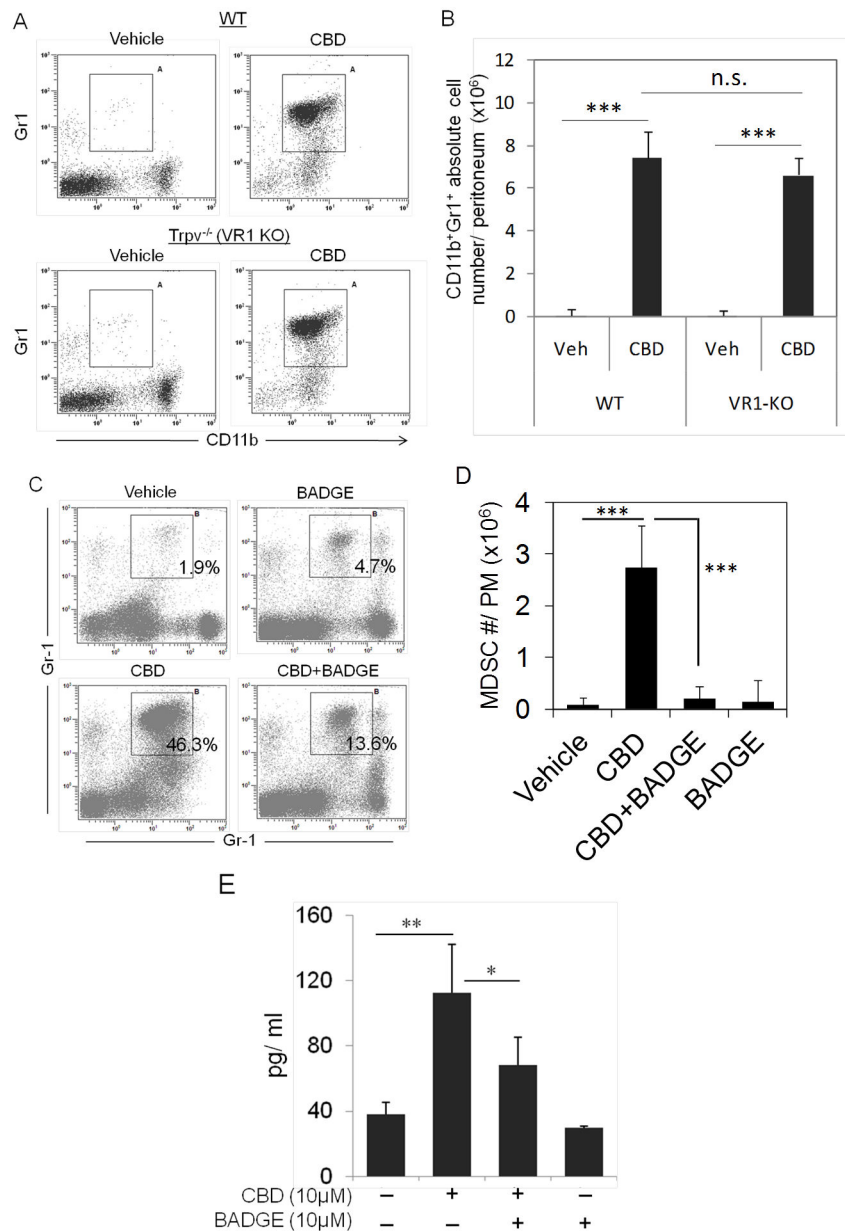


Figure 10. PPAR γ plays a critical role in the induction of MDSC by CBD *in vivo*
 Flow cytometric analysis of MDSC from peritoneum 12 h after injecting with vehicle or CBD in WT or Trpv1^{-/-} (VR1-KO) mice. Frequencies (A) and absolute numbers of MDSC (B) are depicted. Data represent mean \pm SD (n=3 mice). Flow cytometric analysis of MDSC from peritoneum 12 h after injecting with vehicle or CBD in WT mice with or without pretreatment of mice using specific inhibitor (BADGE) to block PPAR γ receptors (C, D). Data represent Mean \pm SD (n=4 mice). Student's *t*-test: ****P*<0.001. E) Murine mast cells secrete G-CSF in response to CBD in a PPAR γ -dependent manner. Normal murine cloned mast cells (MC/9) were treated in culture (10⁶ cells/well) with 1 or 10 μ M CBD. In some wells PPAR γ -inhibitor BADGE was added at 1 or 10 μ M as indicated. Culture supernatants were harvested after 24 h and analyzed for G-CSF by ELISA. Data represent mean \pm SD of

triplicate determinations and representative of two experiments. Student's *t*-test: ** $P < 0.01$, * $P < 0.05$.

Author Manuscript

Author Manuscript

Author Manuscript

Author Manuscript

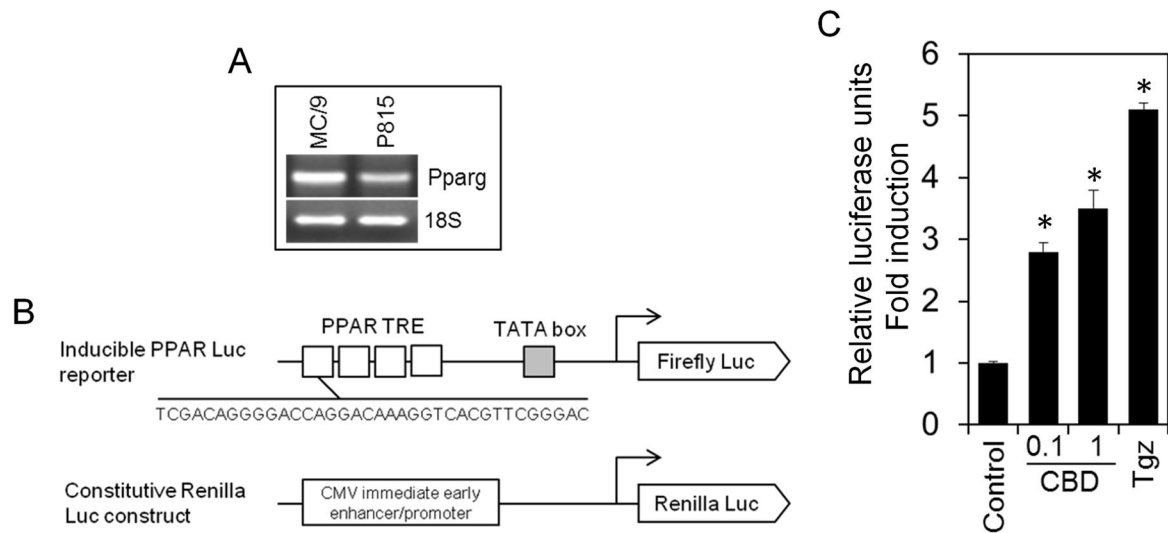


Figure 11. CBD enhances PPAR γ transcriptional activity

A) Expression of PPAR γ on mast cells. PPAR γ message was analyzed on murine cloned mast cells (MC/9) and P815 mast cell line by RT-PCR. B) PPAR γ -luciferase reporter and control vector used in the experiment. Consensus binding site sequence in the PPAR transcriptional response element (TRE) repeats is shown. C) Murine P815 cells were transfected with inducible PPAR-Luciferase (*Firefly*) reporter along with constitutive *Renilla*-luciferase construct followed by treatment with vehicle (control), CBD (0.1 μ M and 1 μ M), or known PPAR γ agonist Troglitazone (10 μ M). Transcriptional activity of PPAR γ was measured by luciferase assay by luminometry. Relative luciferase units were normalized using *Renilla* construct and fold change was calculated. Mean \pm SD of triplicate determinations from a representative experiment are shown. Student's *t*-test, * P <0.05 compared to control.

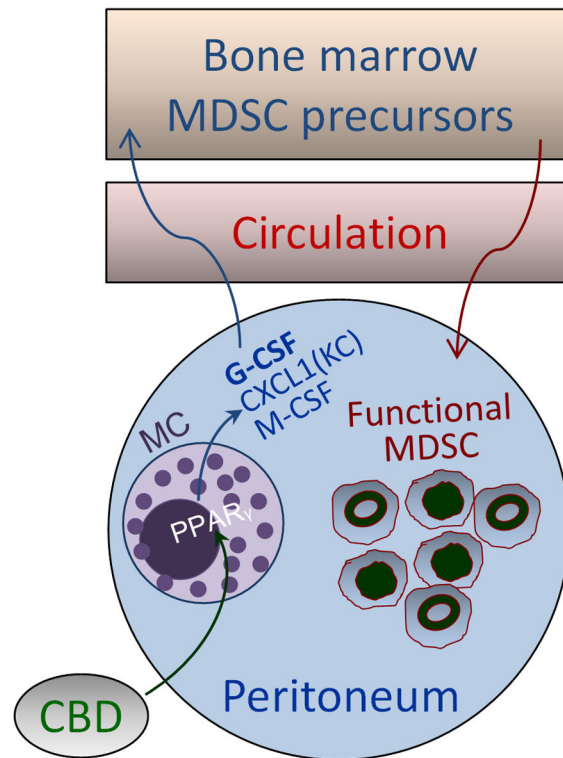


Figure 12. Proposed mechanism induction of MDSC *in vivo* by Cannabidiol

Induction of functional MDSC from BM precursors by CBD and their accumulation in the periphery appears to be primarily mediated by chemokines, predominantly G-CSF with likely involvement of mast cells (MC) and PPAR γ in the process.

Table I

Adoptive transfer of mast cells in mast cell-deficient mice

Mice/treatment	Mast cells in peritoneum*
Control (+/+)	18.79 ± 2.64
Kit (W/W-v)	2.78 ± 1.02
Kit (W/W-v) + BMMC	11.49 ± 3.95

* Mast cells were enumerated using cytopsin preparations of peritoneal lavage cells visualized by May Grünwald Giemsa staining and light microscopy. Mast cells were identified by characteristic deep purple staining of the granules. Number of mast cells and the total number of nucleated cells were counted. Numbers indicate mean ± SD of mast cells per thousand nucleated cells from n=3 mice per group.

Author Manuscript

Author Manuscript

Author Manuscript

Author Manuscript